

The General Relativistic Two Body Problem and the Effective One Body Formalism

Thibault Damour

Abstract A new analytical approach to the motion and radiation of (comparable mass) binary systems has been introduced in 1999 under the name of Effective One Body (EOB) formalism. We review the basic elements of this formalism, and discuss some of its recent developments. Several recent comparisons between EOB predictions and Numerical Relativity (NR) simulations have shown the aptitude of the EOB formalism to provide accurate descriptions of the dynamics and radiation of various binary systems (comprising black holes or neutron stars) in regimes that are inaccessible to other analytical approaches (such as the last orbits and the merger of comparable mass black holes). In synergy with NR simulations, post-Newtonian (PN) theory and Gravitational Self-Force (GSF) computations, the EOB formalism is likely to provide an efficient way of computing the very many accurate template waveforms that are needed for Gravitational Wave (GW) data analysis purposes.

1 Introduction

The general relativistic N -body problem has been investigated from the early days of Einstein's gravitation theory (and even earlier, because it was already tackled by Johannes Droste within the framework of the 1913 Einstein-Grossmann "Entwurf" theory). Here, we shall focus on the general relativistic two-body problem. This problem has been the subject of many investigations within the post-Newtonian (PN) formalism, since the pioneering works of Einstein (1915; when $m_1 \ll m_2$), Lorentz and Droste (1917), Levi-Civita (1937) and Einstein, Infeld and Hoffmann (1938). [see, *e.g.*, [1] for a review and references to the early literature.] For many years, the first post-Newtonian (1PN) approximation (*i.e.* the inclusion of the leading-order relativistic corrections, proportional to $(v/c)^2$ or GM/c^2r , to

Thibault Damour
Institut des Hautes Études Scientifiques, 35 route de Chartres, 91440 Bures-sur-Yvette, France,
e-mail: damour@ihes.fr

the Newtonian equations of motion) appeared as being accurate enough for applying Einstein’s theory to known binary systems. The situation changed in the mid 1970’s with the discovery of the Hulse-Taylor binary pulsar PSR 1913 + 16. The need to compare the accurate observations of this system (by Taylor and collaborators) to the predictions of Einstein’s theory motivated the development of improved relativistic theories of binary systems, applicable to strongly self-gravitating bodies, and including terms up to the 2.5PN approximation (*i.e.* $O[(v/c)^5]$ beyond Newton). [See [2] and references therein.] The situation has again changed recently with the development of interferometric gravitational wave (GW) detectors, and the prospect of detecting the GW’s emitted during the last orbits and the coalescence of binary systems made of black holes or neutron stars. The latter prospect motivated the development (or improvement) of several different methods of computing the motion and radiation of binary systems.

First, this motivated pushing PN calculations of the dynamics of binary systems to the 3PN level [3, 4, 5, 6, 7], with inclusion of 3.5PN radiation-reaction terms [8, 9, 10]. Second, this motivated the development of new, accurate GW generation formalisms, notably the Blanchet-Damour-Iyer (matched) “multipolar post-Minkowskian” formalism [11, 12, 13, 14, 15, 16] and the “direct integration of the relaxed Einstein’s equations” formalism of Will and collaborators [17, 18, 19], which extended previous work by Epstein and Wagoner [20] and Thorne [21]. These GW generation formalisms allowed one to compute emitted gravitational waveforms with an unprecedented PN accuracy¹. After the 1PN correction to the waveform [20, 22, 12], there is a 1.5PN “tail” (*i.e.* hereditary) correction [15, 23, 24], then a “direct” 2PN term [25, 26, 17], followed by higher-order corrections [27, 28, 29, 30, 31, 32, 33, 34, 35]. [See [36] for a detailed account and more references.] Parallely to these improved PN computations of the GW emission of comparable-mass systems (with $m_1 \sim m_2$), other authors developed the analytical theory of the GW emission of extreme mass-ratio systems (with $m_1 \ll m_2$): see Refs. [37, 38, 39, 40] and the review of Sasaki and Tagoshi [41].

Some of the PN calculations of the dynamics, and/or GW emission, of comparable-mass systems have been recently (re)done (e.g. the 3PN dynamics [42]) by using a somewhat different formalism, dubbed “effective field theory” [43]. Let us, however, note that most of the technical aspects of the effective-field-theory approach had already been introduced and used before. For instance: (i) Ref. [44] discussed the (Fokker) two-body effective action due to the exchange of a linear field (of spin $s = 0, 1$ and 2); (ii) Ref. [45] explicitly discussed the representation (and computation) of the (nonlinear) effective two-body action in terms of Feynman-like diagrams (made of concatenated propagators and vertices); (iii) The appendix A of Ref. [46] discussed finite-size effects in terms of nonminimal worldline couplings in the effective action; (iv) The (quantum field theory) technique of dimensional regularization (together with a diagrammatic analysis of ultraviolet divergences) was crucially

¹ For gravitational waveforms, one conventionally defines the PN accuracy as the *fractional* PN accuracy with respect to the leading-order, $O(c^{-5})$, quadrupolar emission. *E.g.*, a 1PN-accurate waveform retains next-to-leading order terms, *i.e.* terms smaller than the quadrupolar waveform by a factor $O(c^{-2})$.

used to derive the 3PN dynamics in Refs. [5, 6], and 3PN radiation in Ref. [31]; and (v) The exponential parametrization of the metric (which suppresses the leading-order gravitational cubic vertex) had been introduced in Ref. [12] and then standardly used in many PN works. It is, however, possible that the more systematic (and automatized) implementation of such diagrammatic methods, together with the tapping of standard techniques for computing Feynman graphs (as exemplified in [42]) may allow one to be more efficient in computing higher-order processes, or, at least, to open new ways of understanding them (see, in this respect, Ref. [47]).

Separately from these purely analytical approaches to the motion and radiation of binary systems, which have been developed since the early days of Einstein's theory, Numerical Relativity (NR) simulations of Einstein's equations have relatively recently (2005) succeeded (after more than thirty years of developmental progress) to stably evolve binary systems made of comparable mass black holes [48, 49, 50, 51]. This has led to an explosion of works exploring many different aspects of strong-field dynamics in General Relativity, such as spin effects, recoil, relaxation of the deformed horizon formed during the coalescence of two black holes to a stationary Kerr black hole, high-velocity encounters, etc.; see [52] for a review. In addition, recently developed codes now allow one to accurately study the orbital dynamics, and the coalescence of binary neutron stars. Much physics remains to be explored in these systems, especially during and after the merger of the neutron stars (which involves a much more complex physics than the pure-gravity merger of two black holes).

Recently, a new source of information on the general relativistic two-body problem has opened: gravitational self-force (GSF) theory. This approach goes one step beyond the test-particle approximation (already used by Einstein in 1915) by taking into account self-field effects that modify the leading-order geodesic motion of a small mass m_1 moving in the background geometry generated by a large mass m_2 . After some ground work (notably by DeWitt and Brehme) in the 1960's, GSF theory has recently undergone rapid developments (mixing theoretical and numerical methods) and can now yield numerical results that yield access to new information on strong-field dynamics in the extreme mass-ratio limit $m_1 \ll m_2$. See Ref. [53] for a review.

Each of the approaches to the two-body problem mentioned so far, PN theory, NR simulations and GSF theory, have their advantages and their drawbacks. It has become recently clear that the best way to meet the challenge of accurately computing the gravitational waveforms (depending on several continuous parameters) that are needed for a successful detection and data analysis of GW signals in the upcoming LIGO/Virgo/GEO/... network of GW detectors is to combine knowledge from all the available approximation methods: PN, NR and GSF. Several ways of doing so are a priori possible. For instance, one could try to directly combine PN-computed waveforms (approximately valid for large enough separations, say $r \gtrsim 10G(m_1 + m_2)/c^2$) with NR waveforms (computed with initial separations $r_0 > 10G(m_1 + m_2)/c^2$ and evolved up to merger and ringdown). However, this

method still requires too much computational time, and is likely to lead to waveforms of rather poor accuracy, see, *e.g.*, [54, 55, 56].

On the other hand, five years before NR succeeded in simulating the late inspiral and the coalescence of binary black holes, a new approach to the two-body problem was proposed: the Effective One Body (EOB) formalism [57, 58, 59, 60]. The basic aim of the EOB formalism is to provide an analytical description of both the motion and the radiation of coalescing binary systems over the entire merger process, from the early inspiral, right through the plunge, merger and final ringdown. As early as 2000 [58] this method made several quantitative and qualitative predictions concerning the dynamics of the coalescence, and the corresponding GW radiation, notably: (i) a blurred transition from inspiral to a ‘plunge’ that is just a smooth continuation of the inspiral, (ii) a sharp transition, around the merger of the black holes, between a continued inspiral and a ring-down signal, and (iii) estimates of the radiated energy and of the spin of the final black hole. In addition, the effects of the individual spins of the black holes were investigated within the EOB [60, 61] and were shown to lead to a larger energy release for spins parallel to the orbital angular momentum, and to a dimensionless rotation parameter J/E^2 always smaller than unity at the end of the inspiral (so that a Kerr black hole can form right after the inspiral phase). All those predictions have been broadly confirmed by the results of the recent numerical simulations performed by several independent groups (for a review of numerical relativity results and references see [52]). Note that, in spite of the high computer power used in NR simulations, the calculation, checking and processing of one sufficiently long waveform (corresponding to specific values of the many continuous parameters describing the two arbitrary masses, the initial spin vectors, and other initial data) takes on the order of one month. This is a very strong argument for developing analytical models of waveforms.

2 EOB description of the conservative dynamics of two body systems

Before reviewing some of the technical aspects of the EOB method, let us indicate the historical roots of this method. First, we note that the EOB approach comprises three, rather separate, ingredients:

1. a description of the conservative (Hamiltonian) part of the dynamics of two bodies;
2. an expression for the radiation-reaction part of the dynamics;
3. a description of the GW waveform emitted by a coalescing binary system.

For each one of these ingredients, the essential inputs that are used in EOB works are high-order post-Newtonian (PN) expanded results which have been obtained by many years of work, by many researchers (see references above). However, one of the key ideas in the EOB philosophy is to avoid using PN results in their original

“Taylor-expanded” form (*i.e.* $c_0 + c_1 v/c + c_2 v^2/c^2 + c_3 v^3/c^3 + \dots + c_n v^n/c^n$), but to use them instead in some *resummed* form (*i.e.* some non-polynomial function of v/c , defined so as to incorporate some of the expected non-perturbative features of the exact result). The basic ideas and techniques for resumming each ingredient of the EOB are different and have different historical roots.

Concerning the first ingredient, *i.e.* the EOB Hamiltonian, it was inspired by an approach to electromagnetically interacting quantum two-body systems introduced by Brézin, Itzykson and Zinn-Justin [62].

The resummation of the second ingredient, *i.e.* the EOB radiation-reaction force \mathcal{F} , was initially inspired by the Padé resummation of the flux function introduced by Damour, Iyer and Sathyaprakash [63]. More recently, a new and more sophisticated resummation technique for the radiation reaction force \mathcal{F} has been introduced by Damour and Nagar [64, 65].

As for the third ingredient, *i.e.* the EOB description of the waveform emitted by a coalescing black hole binary, it was mainly inspired by the work of Davis, Ruffini and Tiomno [66] which discovered the transition between the plunge signal and a ringing tail when a particle falls into a black hole. [Additional motivation for the EOB treatment of the transition from plunge to ring-down came from work on the, so-called, “close limit approximation” [67].] In addition, a very efficient resummation of the waveform has been introduced by Damour, Iyer and Nagar [68, 69, 64]. It will be discussed in detail below.

Within the usual PN formalism, the conservative dynamics of a two-body system is currently fully known up to the 3PN level [3, 4, 5, 6, 7, 42] (see below for the partial knowledge beyond the 3PN level). Going to the center of mass of the system ($\mathbf{p}_1 + \mathbf{p}_2 = 0$), the 3PN-accurate Hamiltonian (in Arnowitt-Deser-Misner-type coordinates) describing the relative motion, $\mathbf{q} = \mathbf{q}_1 - \mathbf{q}_2$, $\mathbf{p} = \mathbf{p}_1 = -\mathbf{p}_2$, has the structure

$$H_{3\text{PN}}^{\text{relative}}(\mathbf{q}, \mathbf{p}) = H_0(\mathbf{q}, \mathbf{p}) + \frac{1}{c^2} H_2(\mathbf{q}, \mathbf{p}) + \frac{1}{c^4} H_4(\mathbf{q}, \mathbf{p}) + \frac{1}{c^6} H_6(\mathbf{q}, \mathbf{p}), \quad (1)$$

where

$$H_0(\mathbf{q}, \mathbf{p}) = \frac{1}{2\mu} \mathbf{p}^2 - \frac{GM\mu}{|\mathbf{q}|}, \quad (2)$$

with

$$M \equiv m_1 + m_2 \quad \text{and} \quad \mu \equiv m_1 m_2 / M, \quad (3)$$

corresponds to the Newtonian approximation to the relative motion, while H_2 describes 1PN corrections, H_4 2PN ones and H_6 3PN ones. In terms of the rescaled variables $\mathbf{q}' \equiv \mathbf{q}/GM$, $\mathbf{p}' \equiv \mathbf{p}/\mu$, the explicit form (after dropping the primes for readability) of the 3PN-accurate rescaled Hamiltonian $\hat{H} \equiv H/\mu$ reads [70, 71, 5]

$$\hat{H}_N(\mathbf{q}, \mathbf{p}) = \frac{\mathbf{p}^2}{2} - \frac{1}{q}, \quad (4)$$

$$\hat{H}_{1\text{PN}}(\mathbf{q}, \mathbf{p}) = \frac{1}{8}(3\nu - 1)(\mathbf{p}^2)^2 - \frac{1}{2}[(3 + \nu)\mathbf{p}^2 + \nu(\mathbf{n} \cdot \mathbf{p})^2] \frac{1}{q} + \frac{1}{2q^2}, \quad (5)$$

$$\begin{aligned} \hat{H}_{2\text{PN}}(\mathbf{q}, \mathbf{p}) &= \frac{1}{16}(1 - 5\nu + 5\nu^2)(\mathbf{p}^2)^3 \\ &+ \frac{1}{8}[(5 - 20\nu - 3\nu^2)(\mathbf{p}^2)^2 - 2\nu^2(\mathbf{n} \cdot \mathbf{p})^2 \mathbf{p}^2 - 3\nu^2(\mathbf{n} \cdot \mathbf{p})^4] \frac{1}{q} \\ &+ \frac{1}{2}[(5 + 8\nu)\mathbf{p}^2 + 3\nu(\mathbf{n} \cdot \mathbf{p})^2] \frac{1}{q^2} - \frac{1}{4}(1 + 3\nu) \frac{1}{q^3}, \end{aligned} \quad (6)$$

$$\begin{aligned} \hat{H}_{3\text{PN}}(\mathbf{q}, \mathbf{p}) &= \frac{1}{128}(-5 + 35\nu - 70\nu^2 + 35\nu^3)(\mathbf{p}^2)^4 \\ &+ \frac{1}{16}[(-7 + 42\nu - 53\nu^2 - 5\nu^3)(\mathbf{p}^2)^3 + (2 - 3\nu)\nu^2(\mathbf{n} \cdot \mathbf{p})^2(\mathbf{p}^2)^2 \\ &\quad + 3(1 - \nu)\nu^2(\mathbf{n} \cdot \mathbf{p})^4 \mathbf{p}^2 - 5\nu^3(\mathbf{n} \cdot \mathbf{p})^6] \frac{1}{q} \\ &+ \left[\frac{1}{16}(-27 + 136\nu + 109\nu^2)(\mathbf{p}^2)^2 + \frac{1}{16}(17 + 30\nu)\nu(\mathbf{n} \cdot \mathbf{p})^2 \mathbf{p}^2 \right. \\ &\quad \left. + \frac{1}{12}(5 + 43\nu)\nu(\mathbf{n} \cdot \mathbf{p})^4 \right] \frac{1}{q^2} \\ &+ \left\{ \left[-\frac{25}{8} + \left(\frac{1}{64}\pi^2 - \frac{335}{48} \right) \nu - \frac{23}{8}\nu^2 \right] \mathbf{p}^2 \right. \\ &\quad \left. + \left(-\frac{85}{16} - \frac{3}{64}\pi^2 - \frac{7}{4}\nu \right) \nu(\mathbf{n} \cdot \mathbf{p})^2 \right\} \frac{1}{q^3} \\ &+ \left[\frac{1}{8} + \left(\frac{109}{12} - \frac{21}{32}\pi^2 \right) \nu \right] \frac{1}{q^4}. \end{aligned} \quad (7)$$

In these formulas ν denotes the symmetric mass ratio:

$$\nu \equiv \frac{\mu}{M} \equiv \frac{m_1 m_2}{(m_1 + m_2)^2}. \quad (8)$$

The dimensionless parameter ν varies between 0 (extreme mass ratio case) and $\frac{1}{4}$ (equal mass case) and plays the rôle of a deformation parameter away from the test-mass limit.

It is well known that, at the Newtonian approximation, $H_0(\mathbf{q}, \mathbf{p})$ can be thought of as describing a ‘test particle’ of mass μ orbiting around an ‘external mass’ GM . The EOB approach is a *general relativistic generalization* of this fact. It consists in looking for an ‘effective external spacetime geometry’ $g_{\mu\nu}^{\text{eff}}(x^\lambda; GM, \nu)$ such that the geodesic dynamics of a ‘test particle’ of mass μ within $g_{\mu\nu}^{\text{eff}}(x^\lambda, GM, \nu)$ is *equivalent* (when expanded in powers of $1/c^2$) to the original, relative PN-expanded dynamics (1).

Let us explain the idea, proposed in [57], for establishing a ‘dictionary’ between the real relative-motion dynamics, (1), and the dynamics of an ‘effective’ particle of mass μ moving in $g_{\mu\nu}^{\text{eff}}(x^\lambda, GM, \mathbf{v})$. The idea consists in ‘thinking quantum mechanically’². Instead of thinking in terms of a classical Hamiltonian, $H(\mathbf{q}, \mathbf{p})$ (such as $H_{\text{3PN}}^{\text{relative}}$, Eq. (1)), and of its classical bound orbits, we can think in terms of the quantized energy levels $E(n, \ell)$ of the quantum bound states of the Hamiltonian operator $H(\hat{\mathbf{q}}, \hat{\mathbf{p}})$. These energy levels will depend on two (integer valued) quantum numbers n and ℓ . Here (for a spherically symmetric interaction, as appropriate to H^{relative}), ℓ parametrizes the total orbital angular momentum ($\mathbf{L}^2 = \ell(\ell + 1)\hbar^2$), while n represents the ‘principal quantum number’ $n = \ell + n_r + 1$, where n_r (the ‘radial quantum number’) denotes the number of nodes in the radial wave function. The third ‘magnetic quantum number’ m (with $-\ell \leq m \leq \ell$) does not enter the energy levels because of the spherical symmetry of the two-body interaction (in the center of mass frame). For instance, the non-relativistic Newton interaction Eq. (2) gives rise to the well-known result

$$E_0(n, \ell) = -\frac{1}{2}\mu \left(\frac{GM\mu}{n\hbar} \right)^2, \quad (9)$$

which depends only on n (this is the famous Coulomb degeneracy). When considering the PN corrections to H_0 , as in Eq. (1), one gets a more complicated expression of the form

$$E_{\text{3PN}}^{\text{relative}}(n, \ell) = -\frac{1}{2}\mu \frac{\alpha^2}{n^2} \left[1 + \frac{\alpha^2}{c^2} \left(\frac{c_{11}}{n\ell} + \frac{c_{20}}{n^2} \right) + \frac{\alpha^4}{c^4} \left(\frac{c_{13}}{n\ell^3} + \frac{c_{22}}{n^2\ell^2} + \frac{c_{31}}{n^3\ell} + \frac{c_{40}}{n^4} \right) + \frac{\alpha^6}{c^6} \left(\frac{c_{15}}{n\ell^5} + \dots + \frac{c_{60}}{n^6} \right) \right], \quad (10)$$

where we have set $\alpha \equiv GM\mu/\hbar = Gm_1 m_2/\hbar$, and where we consider, for simplicity, the (quasi-classical) limit where n and ℓ are large numbers. The 2PN-accurate version of Eq. (10) had been derived by Damour and Schäfer [72] as early as 1988 while its 3PN-accurate version was derived by Damour, Jaranowski and Schäfer in 1999 [70]. The dimensionless coefficients c_{pq} are functions of the symmetric mass ratio $\nu \equiv \mu/M$, for instance $c_{40} = \frac{1}{8}(145 - 15\nu + \nu^2)$. In classical mechanics (*i.e.* for large n and ℓ), it is called the ‘Delaunay Hamiltonian’, *i.e.* the Hamiltonian expressed in terms of the *action variables*³ $J = \ell\hbar = \frac{1}{2\pi} \oint p_\varphi d\varphi$, and $N = n\hbar = I_r + J$, with $I_r = \frac{1}{2\pi} \oint p_r dr$.

The energy levels (10) encode, in a *gauge-invariant* way, the 3PN-accurate relative dynamics of a ‘real’ binary. Let us now consider an auxiliary problem: the ‘effective’ dynamics of one body, of mass μ , following (modulo the Q term discussed below) a geodesic in some \mathbf{v} -dependent ‘effective external’ (spherically symmetric)

² This is related to an idea emphasized many times by John Archibald Wheeler: quantum mechanics can often help us in going to the essence of classical mechanics.

³ We consider, for simplicity, ‘equatorial’ motions with $m = \ell$, *i.e.*, classically, $\theta = \frac{\pi}{2}$.

metric⁴

$$g_{\mu\nu}^{\text{eff}} dx^\mu dx^\nu = -A(R; \nu) c^2 dT^2 + B(R; \nu) dR^2 + R^2 (d\theta^2 + \sin^2 \theta d\varphi^2). \quad (11)$$

Here, the *a priori unknown* metric functions $A(R; \nu)$ and $B(R; \nu)$ will be constructed in the form of expansions in $GM/c^2 R$:

$$\begin{aligned} A(R; \nu) &= 1 + \tilde{a}_1 \frac{GM}{c^2 R} + \tilde{a}_2 \left(\frac{GM}{c^2 R} \right)^2 + \tilde{a}_3 \left(\frac{GM}{c^2 R} \right)^3 + \tilde{a}_4 \left(\frac{GM}{c^2 R} \right)^4 + \dots; \\ B(R; \nu) &= 1 + \tilde{b}_1 \frac{GM}{c^2 R} + \tilde{b}_2 \left(\frac{GM}{c^2 R} \right)^2 + \tilde{b}_3 \left(\frac{GM}{c^2 R} \right)^3 + \dots, \end{aligned} \quad (12)$$

where the dimensionless coefficients \tilde{a}_n, \tilde{b}_n depend on ν . From the Newtonian limit, it is clear that we should set $\tilde{a}_1 = -2$. In addition, as ν can be viewed as a deformation parameter away from the test-mass limit, we require that the effective metric (11) tend to the Schwarzschild metric (of mass M) as $\nu \rightarrow 0$, *i.e.* that

$$A(R; \nu = 0) = 1 - 2GM/c^2 R = B^{-1}(R; \nu = 0).$$

Let us now require that the dynamics of the ‘‘one body’’ μ within the effective metric $g_{\mu\nu}^{\text{eff}}$ be described by an ‘‘effective’’ mass-shell condition of the form

$$g_{\text{eff}}^{\mu\nu} p_\mu^{\text{eff}} p_\nu^{\text{eff}} + \mu^2 c^2 + Q(p_\mu^{\text{eff}}) = 0,$$

where $Q(p)$ is (at least) *quartic* in p . Then by solving (by separation of variables) the corresponding ‘effective’ Hamilton-Jacobi equation

$$g_{\text{eff}}^{\mu\nu} \frac{\partial S_{\text{eff}}}{\partial x^\mu} \frac{\partial S_{\text{eff}}}{\partial x^\nu} + \mu^2 c^2 + Q \left(\frac{\partial S}{\partial x^\mu} \right) = 0,$$

$$S_{\text{eff}} = -\mathcal{E}_{\text{eff}} t + J_{\text{eff}} \varphi + S_{\text{eff}}(R), \quad (13)$$

one can straightforwardly compute (in the quasi-classical, large quantum numbers limit) the effective Delaunay Hamiltonian $\mathcal{E}_{\text{eff}}(N_{\text{eff}}, J_{\text{eff}})$, with $N_{\text{eff}} = n_{\text{eff}} \hbar$, $J_{\text{eff}} = \ell_{\text{eff}} \hbar$ (where $N_{\text{eff}} = J_{\text{eff}} + I_R^{\text{eff}}$, with $I_R^{\text{eff}} = \frac{1}{2\pi} \oint p_R^{\text{eff}} dR$, $p_R^{\text{eff}} = \partial S_{\text{eff}}(R)/dR$). This yields a result of the form

⁴ It is convenient to write the ‘effective metric’ in Schwarzschild-like coordinates. Note that the effective radial coordinate R differs from the two-body ADM-coordinate relative distance $R^{\text{ADM}} = |\mathbf{q}|$. The transformation between the two coordinate systems has been determined in Refs. [57, 59].

$$\begin{aligned}
\mathcal{E}_{\text{eff}}(n_{\text{eff}}, \ell_{\text{eff}}) = & \mu c^2 - \frac{1}{2} \mu \frac{\alpha^2}{n_{\text{eff}}^2} \left[1 + \frac{\alpha^2}{c^2} \left(\frac{c_{11}^{\text{eff}}}{n_{\text{eff}} \ell_{\text{eff}}} + \frac{c_{20}^{\text{eff}}}{n_{\text{eff}}^2} \right) \right. \\
& + \frac{\alpha^4}{c^4} \left(\frac{c_{13}^{\text{eff}}}{n_{\text{eff}} \ell_{\text{eff}}^3} + \frac{c_{22}^{\text{eff}}}{n_{\text{eff}}^2 \ell_{\text{eff}}^2} + \frac{c_{31}^{\text{eff}}}{n_{\text{eff}}^3 \ell_{\text{eff}}} + \frac{c_{40}^{\text{eff}}}{n_{\text{eff}}^4} \right) \\
& \left. + \frac{\alpha^6}{c^6} \left(\frac{c_{15}^{\text{eff}}}{n_{\text{eff}} \ell_{\text{eff}}^5} + \dots + \frac{c_{60}^{\text{eff}}}{n_{\text{eff}}^6} \right) \right], \tag{14}
\end{aligned}$$

where the dimensionless coefficients c_{pq}^{eff} are now functions of the unknown coefficients \tilde{a}_n, \tilde{b}_n entering the looked for ‘external’ metric coefficients (12).

At this stage, one needs to define a ‘dictionary’ between the real (relative) two-body dynamics, summarized in Eq. (10), and the effective one-body one, summarized in Eq. (14). As, on both sides, quantum mechanics tells us that the action variables are quantized in integers ($N_{\text{real}} = n\hbar$, $N_{\text{eff}} = n_{\text{eff}}\hbar$, etc.) it is most natural to identify $n = n_{\text{eff}}$ and $\ell = \ell_{\text{eff}}$. One then still needs a rule for relating the two different energies $E_{\text{real}}^{\text{relative}}$ and \mathcal{E}_{eff} . Ref. [57] proposed to look for a general map between the real energy levels and the effective ones (which, as seen when comparing (10) and (14), cannot be directly identified because they do not include the same rest-mass contribution⁵), namely

$$\begin{aligned}
\frac{\mathcal{E}_{\text{eff}}}{\mu c^2} - 1 = & f\left(\frac{E_{\text{real}}^{\text{relative}}}{\mu c^2}\right) = \frac{E_{\text{real}}^{\text{relative}}}{\mu c^2} \left(1 + \alpha_1 \frac{E_{\text{real}}^{\text{relative}}}{\mu c^2} + \alpha_2 \left(\frac{E_{\text{real}}^{\text{relative}}}{\mu c^2}\right)^2 \right. \\
& \left. + \alpha_3 \left(\frac{E_{\text{real}}^{\text{relative}}}{\mu c^2}\right)^3 + \dots \right). \tag{15}
\end{aligned}$$

The ‘correspondence’ between the real and effective energy levels is illustrated in Fig. 1.

Finally, identifying $\mathcal{E}_{\text{eff}}(n, \ell)/\mu c^2$ to $1 + f(E_{\text{real}}^{\text{relative}}(n, \ell)/\mu c^2)$ yields a system of equations for determining the unknown EOB coefficients $\tilde{a}_n, \tilde{b}_n, \alpha_n$, as well as the three coefficients z_1, z_2, z_3 parametrizing a general 3PN-level quartic mass-shell deformation:

$$Q_{3\text{PN}}(p) = \frac{1}{c^6} \frac{1}{\mu^2} \left(\frac{GM}{R}\right)^2 [z_1 \mathbf{p}^4 + z_2 \mathbf{p}^2 (\mathbf{n} \cdot \mathbf{p})^2 + z_3 (\mathbf{n} \cdot \mathbf{p})^4].$$

[The need for introducing a quartic mass-shell deformation Q only arises at the 3PN level.]

The above system of equations for $\tilde{a}_n, \tilde{b}_n, \alpha_n$ (and z_i at 3PN) was studied at the 2PN level in Ref. [57], and at the 3PN level in Ref. [59]. At the 2PN level it was found that, if one further imposes the natural condition $\tilde{b}_1 = +2$ (so that the lin-

⁵ Indeed $E_{\text{real}}^{\text{total}} = Mc^2 + E_{\text{real}}^{\text{relative}} = Mc^2 + \text{Newtonian terms} + 1\text{PN}/c^2 + \dots$, while $\mathcal{E}_{\text{effective}} = \mu c^2 + N + 1\text{PN}/c^2 + \dots$.

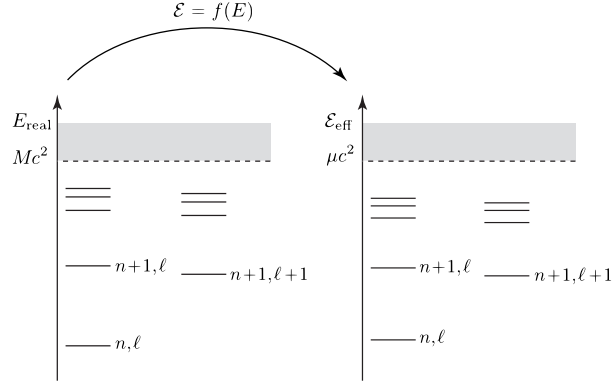


Fig. 1 Sketch of the correspondence between the quantized energy levels of the real and effective conservative dynamics. n denotes the ‘principal quantum number’ ($n = n_r + \ell + 1$, with $n_r = 0, 1, \dots$ denoting the number of nodes in the radial function), while ℓ denotes the (relative) orbital angular momentum ($L^2 = \ell(\ell + 1)\hbar^2$). Though the EOB method is purely classical, it is conceptually useful to think in terms of the underlying (Bohr-Sommerfeld) quantization conditions of the action variables I_R and J to motivate the identification between n and ℓ in the two dynamics.

earized effective metric coincides with the linearized Schwarzschild metric with mass $M = m_1 + m_2$), there exists a *unique* solution for the remaining five unknown coefficients $\tilde{a}_2, \tilde{a}_3, b_2, \alpha_1$ and α_2 . This solution is very simple:

$$\tilde{a}_2 = 0, \quad \tilde{a}_3 = 2\nu, \quad \tilde{b}_2 = 4 - 6\nu, \quad \alpha_1 = \frac{\nu}{2}, \quad \alpha_2 = 0. \quad (16)$$

At the 3PN level, it was found that the system of equations is consistent, and underdetermined in that the general solution can be parametrized by the arbitrary values of z_1 and z_2 . It was then argued that it is natural to impose the simplifying requirements $z_1 = 0 = z_2$, so that Q is proportional to the fourth power of the (effective) radial momentum p_r . With these conditions, the solution is unique at the 3PN level, and is still remarkably simple, namely

$$\tilde{a}_4 = a_4 \nu, \quad \tilde{d}_3 = 2(3\nu - 26)\nu, \quad \alpha_3 = 0, \quad z_3 = 2(4 - 3\nu)\nu.$$

Here, a_4 denotes the number

$$a_4 = \frac{94}{3} - \frac{41}{32}\pi^2 \simeq 18.6879027, \quad (17)$$

while \tilde{d}_3 denotes the coefficient of $(GM/c^2 R)^3$ in the PN expansion of the combined metric coefficient

$$D(R) \equiv A(R)B(R).$$

Replacing $B(R)$ by $D(R)$ is convenient because (as was mentioned above), in the test-mass limit $\nu \rightarrow 0$, the effective metric must reduce to the Schwarzschild metric,

namely

$$A(R; \mathbf{v} = 0) = B^{-1}(R; \mathbf{v} = 0) = 1 - 2 \left(\frac{GM}{c^2 R} \right),$$

so that

$$D(R; \mathbf{v} = 0) = 1.$$

The final result is that the three EOB potentials A, D, Q describing the 3PN two-body dynamics are given by the following very simple results. In terms of the EOB “gravitational potential”

$$u \equiv \frac{GM}{c^2 R},$$

$$A_{3\text{PN}}(R) = 1 - 2u + 2\mathbf{v}u^3 + a_4 \mathbf{v}u^4, \quad (18)$$

$$D_{3\text{PN}}(R) \equiv (A(R)B(R))_{3\text{PN}} = 1 - 6\mathbf{v}u^2 + 2(3\mathbf{v} - 26)\mathbf{v}u^3, \quad (19)$$

$$Q_{3\text{PN}}(\mathbf{q}, \mathbf{p}) = \frac{1}{c^2} 2(4 - 3\mathbf{v})\mathbf{v}u^2 \frac{p_i^4}{\mu^2}. \quad (20)$$

In addition, the map between the (real) center-of-mass energy of the binary system $E_{\text{real}}^{\text{relative}} = H^{\text{relative}} = \mathcal{E}_{\text{relative}}^{\text{tot}} - Mc^2$ and the effective one \mathcal{E}_{eff} is found to have the very simple (but non trivial) form

$$\frac{\mathcal{E}_{\text{eff}}}{\mu c^2} = 1 + \frac{E_{\text{real}}^{\text{relative}}}{\mu c^2} \left(1 + \frac{\mathbf{v}}{2} \frac{E_{\text{real}}^{\text{relative}}}{\mu c^2} \right) = \frac{s - m_1^2 c^4 - m_2^2 c^4}{2m_1 m_2 c^4} \quad (21)$$

where $s = (\mathcal{E}_{\text{real}}^{\text{tot}})^2 \equiv (Mc^2 + E_{\text{real}}^{\text{relative}})^2$ is Mandelstam’s invariant $s = -(p_1 + p_2)^2$.

It is truly remarkable that the EOB formalism succeeds in *condensing* the complicated, original 3PN Hamiltonian, Eqs. (4)–(2), into the very simple potentials A, D and Q displayed above, together with the simple energy map Eq. (21). For instance, at the 1PN level, the already somewhat involved Lorentz-Droste-Einstein-Infeld-Hoffmann 1PN dynamics (Eqs. (4) and (5)) is simply described, within the EOB formalism, as a test particle of mass μ moving in an external Schwarzschild background of mass $M = m_1 + m_2$, together with the (crucial but quite simple) energy transformation (21). [Indeed, the \mathbf{v} -dependent corrections to A and D start only at the 2PN level.] At the 2PN level, the seven rather complicated \mathbf{v} -dependent coefficients of $\widehat{H}_{2\text{PN}}(\mathbf{q}, \mathbf{p})$, Eq. (6), get condensed into the two very simple additional contributions $+2\mathbf{v}u^3$ in $A(u)$, and $-6\mathbf{v}u^2$ in $D(u)$. At the 3PN level, the eleven quite complicated \mathbf{v} -dependent coefficients of $\widehat{H}_{3\text{PN}}$, Eq. (2), get condensed into only three simple contributions: $+a_4 \mathbf{v}u^4$ in $A(u)$, $+2(3\mathbf{v} - 26)\mathbf{v}u^3$ in $D(u)$, and $Q_{3\text{PN}}$ given by Eq. (20). This simplicity of the EOB results is not only due to the reformulation of the PN-expanded Hamiltonian into an effective dynamics. Indeed, the A -potential happens to be much simpler that it could a priori have been: (i) as already noted it is not modified at the 1PN level, while one would a priori expect to have found a

1PN potential $A_{1\text{PN}}(u) = 1 - 2u + \nu a_2 u^2$ with some non zero a_2 ; and (ii) there are striking cancellations taking place in the calculation of the 2PN and 3PN coefficients $\tilde{a}_2(\nu)$ and $\tilde{a}_3(\nu)$, which were a priori of the form $\tilde{a}_2(\nu) = a_2 \nu + a'_2 \nu^2$, and $\tilde{a}_3(\nu) = a_3 \nu + a'_3 \nu^2 + a''_3 \nu^3$, but for which the ν -nonlinear contributions $a'_2 \nu^2$, $a'_3 \nu^2$ and $a''_3 \nu^3$ precisely cancelled out.

The fact that the 3PN coefficient a_4 in the crucial ‘effective radial potential’ $A_{3\text{PN}}(R)$, Eq. (18), is rather large and positive indicates that the ν -dependent nonlinear gravitational effects lead, for comparable masses ($\nu \sim \frac{1}{4}$), to a last stable (circular) orbit (LSO) which has a higher frequency and a larger binding energy than what a naive scaling from the test-particle limit ($\nu \rightarrow 0$) would suggest. Actually, the PN-expanded form (18) of $A_{3\text{PN}}(R)$ does not seem to be a good representation of the (unknown) exact function $A_{\text{EOB}}(R)$ when the (Schwarzschild-like) relative coordinate R becomes smaller than about $6GM/c^2$ (which is the radius of the LSO in the test-mass limit). By continuity with the test-mass case, one a priori expects that $A_{3\text{PN}}(R)$ always exhibits a simple zero defining an EOB ‘‘effective horizon’’ that is smoothly connected to the Schwarzschild event horizon at $R = 2GM/c^2$ when $\nu \rightarrow 0$. However, the large value of the a_4 coefficient does actually prevent $A_{3\text{PN}}$ to have this property when ν is too large, and in particular when $\nu = 1/4$. It was therefore suggested [59] to further resum⁶ $A_{3\text{PN}}(R)$ by replacing it by a suitable Padé (P) approximant. For instance, the replacement of $A_{3\text{PN}}(R)$ by⁷

$$A_3^1(R) \equiv P_3^1[A_{3\text{PN}}(R)] = \frac{1 + n_1 u}{1 + d_1 u + d_2 u^2 + d_3 u^3} \quad (22)$$

ensures that the $\nu = \frac{1}{4}$ case is smoothly connected with the $\nu = 0$ limit.

The same kind of ν -continuity argument, discussed so far for the A function, needs to be applied also to the $D_{3\text{PN}}(R)$ function defined in Eq. (19). A straightforward way to ensure that the D function stays positive when R decreases (since it is $D = 1$ when $\nu \rightarrow 0$) is to replace $D_{3\text{PN}}(R)$ by $D_3^0(R) \equiv P_3^0[D_{3\text{PN}}(R)]$, where P_3^0 indicates the (0, 3) Padé approximant and explicitly reads

$$D_3^0(R) = \frac{1}{1 + 6\nu u^2 - 2(3\nu - 26)\nu u^3}. \quad (23)$$

⁶ The PN-expanded EOB building blocks $A_{3\text{PN}}(R), B_{3\text{PN}}(R), \dots$ already represent a *resummation* of the PN dynamics in the sense that they have ‘‘condensed’’ the many terms of the original PN-expanded Hamiltonian within a very concise format. But one should not refrain to further resum the EOB building blocks themselves, if this is physically motivated.

⁷ We recall that the coefficients n_1 and (d_1, d_2, d_3) of the (1, 3) Padé approximant $P_3^1[A_{3\text{PN}}(u)]$ are determined by the condition that the first four terms of the Taylor expansion of A_3^1 in powers of $u = GM/(c^2 R)$ coincide with $A_{3\text{PN}}$.

3 EOB description of radiation reaction and of the emitted waveform during inspiral

In the previous Section we have described how the EOB method encodes the conservative part of the relative orbital dynamics into the dynamics of an 'effective' particle. Let us now briefly discuss how to complete the EOB dynamics by defining some *resummed* expressions describing radiation reaction effects, and the corresponding waveform emitted at infinity. One is interested in circularized binaries, which have lost their initial eccentricity under the influence of radiation reaction. For such systems, it is enough (in first approximation [58]; see, however, the recent results of Bini and Damour [73]) to include a radiation reaction force in the P_φ equation of motion only. More precisely, we are using phase space variables $R, P_R, \varphi, P_\varphi$ associated to polar coordinates (in the equatorial plane $\theta = \frac{\pi}{2}$). Actually it is convenient to replace the radial momentum P_R by the momentum conjugate to the 'tortoise' radial coordinate $R_* = \int dR(B/A)^{1/2}$, i.e. $P_{R_*} = (A/B)^{1/2} P_R$. The real EOB Hamiltonian is obtained by first solving Eq. (21) to get $H_{\text{real}}^{\text{total}} = \sqrt{s}$ in terms of \mathcal{E}_{eff} , and then by solving the effective Hamilton-Jacobi equation to get \mathcal{E}_{eff} in terms of the effective phase space coordinates \mathbf{q}_{eff} and \mathbf{p}_{eff} . The result is given by two nested square roots (we henceforth set $c = 1$):

$$\hat{H}_{\text{EOB}}(r, p_{r_*}, \varphi) = \frac{H_{\text{EOB}}^{\text{real}}}{\mu} = \frac{1}{v} \sqrt{1 + 2v(\hat{H}_{\text{eff}} - 1)}, \quad (24)$$

where

$$\hat{H}_{\text{eff}} = \sqrt{p_{r_*}^2 + A(r) \left(1 + \frac{p_\varphi^2}{r^2} + z_3 \frac{p_{r_*}^4}{r^2} \right)}, \quad (25)$$

with $z_3 = 2v(4 - 3v)$. Here, we are using suitably rescaled dimensionless (effective) variables: $r = R/GM$, $p_{r_*} = P_{R_*}/\mu$, $p_\varphi = P_\varphi/\mu GM$, as well as a rescaled time $t = T/GM$. This leads to equations of motion for $(r, \varphi, p_{r_*}, p_\varphi)$ of the form

$$\frac{d\varphi}{dt} = \frac{\partial \hat{H}_{\text{EOB}}}{\partial p_\varphi} \equiv \Omega, \quad (26)$$

$$\frac{dr}{dt} = \left(\frac{A}{B}\right)^{1/2} \frac{\partial \hat{H}_{\text{EOB}}}{\partial p_{r_*}}, \quad (27)$$

$$\frac{dp_\varphi}{dt} = \hat{\mathcal{F}}_\varphi, \quad (28)$$

$$\frac{dp_{r_*}}{dt} = - \left(\frac{A}{B}\right)^{1/2} \frac{\partial \hat{H}_{\text{EOB}}}{\partial r}, \quad (29)$$

which explicitly read

$$\frac{d\varphi}{dt} = \frac{Ap_\varphi}{\nu r^2 \widehat{H} \widehat{H}_{\text{eff}}} \equiv \Omega, \quad (30)$$

$$\frac{dr}{dt} = \left(\frac{A}{B}\right)^{1/2} \frac{1}{\nu \widehat{H} \widehat{H}_{\text{eff}}} \left(p_{r_*} + z_3 \frac{2A}{r^2} p_{r_*}^3 \right), \quad (31)$$

$$\frac{dp_\varphi}{dt} = \widehat{\mathcal{F}}_\varphi, \quad (32)$$

$$\frac{dp_{r_*}}{dt} = -\left(\frac{A}{B}\right)^{1/2} \frac{1}{2\nu \widehat{H} \widehat{H}_{\text{eff}}} \left\{ A' + \frac{p_\varphi^2}{r^2} \left(A' - \frac{2A}{r} \right) + z_3 \left(\frac{A'}{r^2} - \frac{2A}{r^3} \right) p_{r_*}^4 \right\}, \quad (33)$$

where $A' = dA/dr$. As explained above the EOB metric function $A(r)$ is defined by Padé resumming the Taylor-expanded result (12) obtained from the matching between the real and effective energy levels (as we were mentioning, one uses a similar Padé resumming for $D(r) \equiv A(r)B(r)$). One similarly needs to resum $\widehat{\mathcal{F}}_\varphi$, i.e., the φ component of the radiation reaction which has been introduced on the r.h.s. of Eq. (28).

Several methods have been tried during the development of the EOB formalism to resum the radiation reaction $\widehat{\mathcal{F}}_\varphi$ (starting from the high-order PN-expanded results that have been obtained in the literature; see references in the Introduction above). Here, we shall briefly explain the new, *parameter-free* resumimation technique for the multipolar waveform (and thus for the energy flux) introduced in Ref. [68, 69] and perfected in [64]. To be precise, the new results discussed in Ref. [64] are twofold: on the one hand, that work generalized the $\ell = m = 2$ *resummed factorized waveform* of [68, 69] to higher multipoles by using the most accurate currently known PN-expanded results [34, 33, 35] as well as the higher PN terms which are known in the test-mass limit [39, 40]; on the other hand, it introduced a *further resumimation procedure* which consists in considering a new theoretical quantity, denoted as $\rho_{\ell m}(x)$, which enters the (ℓ, m) waveform (together with other building blocks, see below) only through its ℓ -th power: $h_{\ell m} \propto (\rho_{\ell m}(x))^\ell$. Here, and below, x denotes the invariant PN-ordering parameter given during inspiral by $x \equiv (GM\Omega/c^3)^{2/3}$.

The main novelty introduced by Refs. [68, 69, 64] is to write the (ℓ, m) multipolar waveform emitted by a circular nonspinning compact binary as the *product* of several factors, namely

$$h_{\ell m}^{(\varepsilon)} = \frac{GM\nu}{c^2 R} n_{\ell m}^{(\varepsilon)} c_{l+\varepsilon}(\nu) x^{(\ell+\varepsilon)/2} Y^{\ell-\varepsilon, -m} \left(\frac{\pi}{2}, \Phi \right) \widehat{S}_{\text{eff}}^{(\varepsilon)} T_{\ell m} e^{i\delta_{\ell m}} \rho_{\ell m}^\ell. \quad (34)$$

Here ε denotes the parity of $\ell + m$ ($\varepsilon = \pi(\ell + m)$), i.e. $\varepsilon = 0$ for “even-parity” (mass-generated) multipoles ($\ell + m$ even), and $\varepsilon = 1$ for “odd-parity” (current-generated) ones ($\ell + m$ odd); $n_{\ell m}^{(\varepsilon)}$ and $c_{l+\varepsilon}(\nu)$ are numerical coefficients; $\widehat{S}_{\text{eff}}^{(\varepsilon)}$ is a μ -normalized effective source (whose definition comes from the EOB formalism); $T_{\ell m}$ is a resummed version [68, 69] of an infinite number of “leading logarithms” entering the

tail effects [15, 27]; $\delta_{\ell m}$ is a supplementary phase (which corrects the phase effects not included in the *complex* tail factor $T_{\ell m}$), and, finally, $(\rho_{\ell m})^\ell$ denotes the ℓ -th power of the quantity $\rho_{\ell m}$ which is the new building block introduced in [64]. Note that in previous papers [68, 69] the quantity $(\rho_{\ell m})^\ell$ was denoted as $f_{\ell m}$ and we will often use this notation below. Before introducing explicitly the various elements entering the waveform (34) it is convenient to decompose $h_{\ell m}$ as

$$h_{\ell m}^{(\varepsilon)} = h_{\ell m}^{(N,\varepsilon)} \hat{h}_{\ell m}^{(\varepsilon)}, \quad (35)$$

where $h_{\ell m}^{(N,\varepsilon)}$ is the Newtonian contribution (*i.e.* the product of the first five factors in Eq. (34)) and

$$\hat{h}_{\ell m}^{(\varepsilon)} \equiv \hat{S}_{\text{eff}}^{(\varepsilon)} T_{\ell m} e^{i\delta_{\ell m}} f_{\ell m} \quad (36)$$

represents a resummed version of all the PN corrections. The PN correcting factor $\hat{h}_{\ell m}^{(\varepsilon)}$, as well as all its building blocks, has the structure $\hat{h}_{\ell m}^{(\varepsilon)} = 1 + \mathcal{O}(x)$.

The reader will find in Ref. [64] the definitions of the quantities entering the ‘‘Newtonian’’ waveform $h_{\ell m}^{(N,\varepsilon)}$, as well as the precise definition of the effective source factor $\hat{S}_{\text{eff}}^{(\varepsilon)}$, which constitutes the first factor in the PN-correcting factor $\hat{h}_{\ell m}^{(\varepsilon)}$. Let us only note here that the definition of $\hat{S}_{\text{eff}}^{(\varepsilon)}$ makes use of EOB-defined quantities. For instance, for even-parity waves ($\varepsilon = 0$) $\hat{S}_{\text{eff}}^{(0)}$ is defined as the μ -scaled *effective* energy $\mathcal{E}_{\text{eff}}/\mu c^2$. [We use the ‘‘ J -factorization’’ definition of $\hat{S}_{\text{eff}}^{(\varepsilon)}$ when $\varepsilon = 1$, *i.e.* for odd parity waves.]

The second building block in the factorized decomposition is the ‘‘tail factor’’ $T_{\ell m}$ (introduced in Refs. [68, 69]). As mentioned above, $T_{\ell m}$ is a resummed version of an infinite number of ‘‘leading logarithms’’ entering the transfer function between the near-zone multipolar wave and the far-zone one, due to *tail effects* linked to its propagation in a Schwarzschild background of mass $M_{\text{ADM}} = H_{\text{EOB}}^{\text{real}}$. Its explicit expression reads

$$T_{\ell m} = \frac{\Gamma(\ell + 1 - 2i\hat{k})}{\Gamma(\ell + 1)} e^{\pi\hat{k}} e^{2i\hat{k}\log(2kr_0)}, \quad (37)$$

where $r_0 = 2GM/\sqrt{e}$ and $\hat{k} \equiv GH_{\text{EOB}}^{\text{real}} m\Omega$ and $k \equiv m\Omega$. Note that \hat{k} differs from k by a rescaling involving the *real* (rather than the *effective*) EOB Hamiltonian, computed at this stage along the sequence of circular orbits.

The tail factor $T_{\ell m}$ is a complex number which already takes into account some of the dephasing of the partial waves as they propagate out from the near zone to infinity. However, as the tail factor only takes into account the leading logarithms, one needs to correct it by a complementary dephasing term, $e^{i\delta_{\ell m}}$, linked to subleading logarithms and other effects. This subleading phase correction can be computed as being the phase $\delta_{\ell m}$ of the complex ratio between the PN-expanded $\hat{h}_{\ell m}^{(\varepsilon)}$ and the above defined source and tail factors. In the comparable-mass case ($\nu \neq 0$), the 3PN δ_{22} phase correction to the leading quadrupolar wave was originally computed in

Ref. [69] (see also Ref. [68] for the $\nu = 0$ limit). Full results for the subleading partial waves to the highest possible PN-accuracy by starting from the currently known 3PN-accurate ν -dependent waveform [35] have been obtained in [64]. For higher-order test-mass ($\nu \rightarrow 0$) contributions, see [74, 75]. For extensions of the (non spinning) factorized waveform of [64] see [76, 77, 78].

The last factor in the multiplicative decomposition of the multipolar waveform can be computed as being the modulus $f_{\ell m}$ of the complex ratio between the PN-expanded $\hat{h}_{\ell m}^{(\varepsilon)}$ and the above defined source and tail factors. In the comparable mass case ($\nu \neq 0$), the f_{22} modulus correction to the leading quadrupolar wave was computed in Ref. [69] (see also Ref. [68] for the $\nu = 0$ limit). For the subleading partial waves, Ref. [64] explicitly computed the other $f_{\ell m}$'s to the highest possible PN-accuracy by starting from the currently known 3PN-accurate ν -dependent waveform [35]. In addition, as originally proposed in Ref. [69], to reach greater accuracy the $f_{\ell m}(x; \nu)$'s extracted from the 3PN-accurate $\nu \neq 0$ results are completed by adding higher order contributions coming from the $\nu = 0$ results [39, 40]. In the particular f_{22} case discussed in [69], this amounted to adding 4PN and 5PN $\nu = 0$ terms. This ‘‘hybridization’’ procedure was then systematically pursued for all the other multipoles, using the 5.5PN accurate calculation of the multipolar decomposition of the gravitational wave energy flux of Refs. [39, 40].

The decomposition of the total PN-correction factor $\hat{h}_{\ell m}^{(\varepsilon)}$ into several factors is in itself a resummation procedure which already improves the convergence of the PN series one has to deal with: indeed, one can see that the coefficients entering increasing powers of x in the PN expansion of the $f_{\ell m}$'s tend to be systematically smaller than the coefficients appearing in the usual PN expansion of $\hat{h}_{\ell m}^{(\varepsilon)}$. The reason for this is essentially twofold: (i) the factorization of $T_{\ell m}$ has absorbed powers of $m\pi$ which contributed to make large coefficients in $\hat{h}_{\ell m}^{(\varepsilon)}$, and (ii) the factorization of either \hat{H}_{eff} or \hat{j} has (in the $\nu = 0$ case) removed the presence of an inverse square-root singularity located at $x = 1/3$ which caused the coefficient of x^n in any PN-expanded quantity to grow as 3^n as $n \rightarrow \infty$.

To further improve the convergence of the waveform several resummations of the factor $f_{\ell m}(x) = 1 + c_1^{\ell m}x + c_2^{\ell m}x^2 + \dots$ have been suggested. First, Refs. [68, 69] proposed to further resum the $f_{22}(x)$ function via a Padé (3,2) approximant, $P_2^3\{f_{22}(x; \nu)\}$, so as to improve its behavior in the strong-field-fast-motion regime. Such a resummation gave an excellent agreement with numerically computed waveforms, near the end of the inspiral and during the beginning of the plunge, for different mass ratios [68, 79, 80]. As we were mentioning above, a new route for resumming $f_{\ell m}$ was explored in Ref. [64]. It is based on replacing $f_{\ell m}$ by its ℓ -th root, say

$$\rho_{\ell m}(x; \nu) = [f_{\ell m}(x; \nu)]^{1/\ell}. \quad (38)$$

The basic motivation for replacing $f_{\ell m}$ by $\rho_{\ell m}$ is the following: the leading ‘‘Newtonian-level’’ contribution to the waveform $h_{\ell m}^{(\varepsilon)}$ contains a factor $\omega^\ell r_{\text{harm}}^\ell \nu^\varepsilon$ where r_{harm} is the harmonic radial coordinate used in the MPM formalism [12, 14]. When computing the PN expansion of this factor one has to insert the PN expansion of the

(dimensionless) harmonic radial coordinate r_{harm} , $r_{\text{harm}} = x^{-1}(1 + c_1x + \mathcal{O}(x^2))$, as a function of the gauge-independent frequency parameter x . The PN re-expansion of $[r_{\text{harm}}(x)]^\ell$ then generates terms of the type $x^{-\ell}(1 + \ell c_1x + \dots)$. This is one (though not the only one) of the origins of 1PN corrections in $h_{\ell m}$ and $f_{\ell m}$ whose coefficients grow linearly with ℓ . The study of [64] has pointed out that these ℓ -growing terms are problematic for the accuracy of the PN-expansions. The replacement of $f_{\ell m}$ by $\rho_{\ell m}$ is a cure for this problem.

Several studies, both in the test-mass limit, $v \rightarrow 0$ (see Fig. 1 in [64]) and in the comparable-mass case (see notably Fig. 4 in [65]), have shown that the resummed factorized (inspiral) EOB waveforms defined above provided remarkably accurate analytical approximations to the “exact” inspiral waveforms computed by numerical simulations. These resummed multipolar EOB waveforms are much closer (especially during late inspiral) to the exact ones than the standard PN-expanded waveforms given by Eq. (35) with a PN-correction factor of the usual “Taylor-expanded” form

$$\widehat{h}_{\ell m}^{(\varepsilon)\text{PN}} = 1 + c_1^{\ell m}x + c_{3/2}^{\ell m}x^{3/2} + c_2^{\ell m}x^2 + \dots$$

See Fig. 1 in [64], and slide 29 in my (June 2012) Prague presentation.

Finally, one uses the newly resummed multipolar waveforms (34) to define a resummation of the *radiation reaction force* \mathcal{F}_φ as

$$\mathcal{F}_\varphi \equiv -\frac{1}{\Omega}F^{(\ell_{\text{max}})}, \quad (39)$$

where the (instantaneous, circular) GW flux $F^{(\ell_{\text{max}})}$ is defined as

$$F^{(\ell_{\text{max}})} \equiv \frac{2}{16\pi G} \sum_{\ell=2}^{\ell_{\text{max}}} \sum_{m=1}^{\ell} (m\Omega)^2 |Rh_{\ell m}|^2. \quad (40)$$

Summarizing: Eqs. (34) and (39), (40) define resummed EOB versions of the waveform $h_{\ell m}$, and of the radiation reaction $\widehat{\mathcal{F}}_\varphi$, during inspiral. A crucial point is that these resummed expressions are *parameter-free*. Given some current approximation to the conservative EOB dynamics (*i.e.* some expressions for the A, D, Q potentials) they *complete* the EOB formalism by giving explicit predictions for the radiation reaction (thereby completing the dynamics, see Eqs. (26)–(29)), and for the emitted inspiral waveform.

4 EOB description of the merger of binary black holes and of the ringdown of the final black hole

Up to now we have reviewed how the EOB formalism, starting only from *analytical* information obtained from PN theory, and adding extra resummation requirements (both for the EOB conservative potentials A , Eq. (22), and D , Eq. (23), and

for the waveform, Eq. (34), and its associated radiation reaction force, Eqs. (39), (40)) makes specific predictions, both for the motion and the radiation of binary black holes. The analytical calculations underlying such an EOB description are essentially based on skeletonizing the two black holes as two, sufficiently separated point masses, and therefore seem unable to describe the merger of the two black holes, and the subsequent ringdown of the final, single black hole formed during the merger. However, as early as 2000 [58], the EOB formalism went one step further and proposed a specific strategy for describing the *complete* waveform emitted during the entire coalescence process, covering inspiral, merger and ringdown. This EOB proposal is somewhat crude. However, the predictions it has made (years before NR simulations could accurately describe the late inspiral and merger of binary black holes) have been broadly confirmed by subsequent NR simulations. [See the Introduction for a list of EOB predictions.] The original EOB proposal (which was motivated partly by the closeness between the 2PN-accurate effective metric $g_{\mu\nu}^{\text{eff}}$ [57] and the Schwarzschild metric, and by the results of Refs. [66] and [67]) consists of:

(i) defining, within EOB theory, the instant of (effective) “merger” of the two black holes as the (dynamical) EOB time t_m where the orbital frequency $\Omega(t)$ reaches its *maximum*;

(ii) describing (for $t \leq t_m$) the inspiral-plus-plunge (or simply *insplunge*) waveform, $h_{\ell m}^{\text{insplunge}}(t)$, by using the inspiral EOB dynamics and waveform reviewed in the previous Section; and

(iii) describing (for $t \geq t_m$) the merger-plus-ringdown waveform as a superposition of several quasi-normal-mode (QNM) complex frequencies of a final Kerr black hole (of mass M_f and spin parameter a_f , self-consistency estimated within the EOB formalism), say

$$\left(\frac{Rc^2}{GM}\right) h_{\ell m}^{\text{ringdown}}(t) = \sum_N C_N^+ e^{-\sigma_N^+(t-t_m)}, \quad (41)$$

with $\sigma_N^+ = \alpha_N + i\omega_N$, and where the label N refers to indices (ℓ, ℓ', m, n) , with (ℓ, m) being the Schwarzschild-background multipolarity of the considered (metric) waveform $h_{\ell m}$, with $n = 0, 1, 2, \dots$ being the ‘overtone number’ of the considered Kerr-background Quasi-Normal-Mode, and ℓ' the degree of its associated spheroidal harmonics $S_{\ell' m}(a\sigma, \theta)$;

(iv) determining the excitation coefficients C_N^+ of the QNM’s in Eq. (41) by using a simplified representation of the transition between plunge and ring-down obtained by smoothly *matching* (following Ref. [68]), on a $(2p+1)$ -toothed “comb” ($t_m - p\delta, \dots, t_m - \delta, t_m, t_m + \delta, \dots, t_m + p\delta$) centered around the merger (and matching) time t_m , the inspiral-plus-plunge waveform to the above ring-down waveform.

Finally, one defines a complete, quasi-analytical EOB waveform (covering the full process from inspiral to ring-down) as:

$$h_{\ell m}^{\text{EOB}}(t) = \theta(t_m - t) h_{\ell m}^{\text{insplunge}}(t) + \theta(t - t_m) h_{\ell m}^{\text{ringdown}}(t), \quad (42)$$

where $\theta(t)$ denotes Heaviside's step function. The final result is a waveform that essentially depends only on the choice of a resummed EOB $A(u)$ potential, and, less importantly, on the choice of resummation of the main waveform amplitude factor $f_{22} = (\rho_{22})^2$.

We have emphasized here that the EOB formalism is able, in principle, starting only from the best currently known analytical information, to predict the full waveform emitted by coalescing binary black holes. The early comparisons between 3PN-accurate EOB predicted waveforms⁸ and NR-computed waveforms showed a satisfactory agreement between the two, within the (then relatively large) NR uncertainties [81, 82]. Moreover, as we shall discuss below, it has been recently shown that the currently known Padé-resummed 3PN-accurate $A(u)$ potential is able, as is, to describe with remarkable accuracy several aspects of the dynamics of coalescing binary black holes, [83, 84].

On the other hand, when NR started delivering high-accuracy waveforms, it became clear that the 3PN-level analytical knowledge incorporated in EOB theory was not accurate enough for providing waveforms agreeing with NR ones within the high-accuracy needed for detection, and data analysis of upcoming GW signals. [See, *e.g.*, the discussion in Section II of Ref. [77].] At that point, one made use of the *natural flexibility* of the EOB formalism. Indeed, as already emphasized in early EOB work [60, 85], we know from the analytical point of view that there are (yet uncalculated) further terms in the u -expansions of the EOB potentials $A(u), D(u), \dots$ (and in the x -expansion of the waveform), so that these terms can be introduced either as “free parameter(s) in constructing a bank of templates, and [one should] wait until” GW observations determine their value(s) [60], or as “*fitting parameters* and adjusted so as to reproduce other information one has about the exact results” (to quote Ref. [85]). For instance, modulo logarithmic corrections that will be further discussed below, the Taylor expansion in powers of u of the main EOB potential $A(u)$ reads

$$A^{\text{Taylor}}(u; \nu) = 1 - 2u + \tilde{a}_3(\nu)u^3 + \tilde{a}_4(\nu)u^4 + \tilde{a}_5(\nu)u^5 + \tilde{a}_6(\nu)u^6 + \dots$$

where the 2PN and 3PN coefficients $\tilde{a}_3(\nu) = 2\nu$ and $\tilde{a}_4(\nu) = a_4\nu$ are known, but where the 4PN, 5PN, \dots coefficients, $\tilde{a}_5(\nu), \tilde{a}_6(\nu), \dots$ have not yet been calculated (see, however, below). A first attempt was made in [85] to use numerical data (on circular orbits of corotating black holes) to fit the value of a (single, effective) 4PN parameter of the simple form $\tilde{a}_5(\nu) = a_5\nu$ entering a Padé-resummed 4PN-level A potential, *i.e.*

$$A_4^1(u; a_5, \nu) = P_4^1 \left[A_{3\text{PN}}(u) + \nu a_5 u^5 \right]. \quad (43)$$

This strategy was pursued in Ref. [86, 69] and many subsequent works. It was pointed out in Ref. [65] that the introduction of a further 5PN coefficient $\tilde{a}_6(\nu) =$

⁸ The new, resummed EOB waveform discussed above was not available at the time, so that these comparisons employed the coarser “Newtonian-level” EOB waveform $h_{22}^{(N,\varepsilon)}(x)$.

$a_6 v$, entering a Padé-resummed 5PN-level A potential, *i.e.*

$$A_5^1(u; a_5, a_6, v) = P_5^1 \left[A_{3\text{PN}}(u) + v a_5 u^5 + v a_6 u^6 \right], \quad (44)$$

helped in having a closer agreement with accurate NR waveforms.

In addition, Refs. [68, 69] introduced another type of flexibility parameters of the EOB formalism: the non quasi-circular (NQC) parameters accounting for uncalculated modifications of the quasi-circular inspiral waveform presented above, linked to deviations from an adiabatic quasi-circular motion. These NQC parameters are of various types, and subsequent works [79, 80, 65, 87, 88, 89, 77] have explored several ways of introducing them. They enter the EOB waveform in two separate ways. First, through an explicit, additional complex factor multiplying $h_{\ell m}$, *e.g.*

$$f_{\ell m}^{\text{NQC}} = (1 + a_1^{\ell m} n_1 + a_2^{\ell m} n_2) \exp[i(a_3^{\ell m} n_3 + a_4^{\ell m} n_4)]$$

where the n_i 's are dynamical functions that vanish in the quasi-circular limit (with n_1, n_2 being time-even, and n_3, n_4 time-odd). For instance, one usually takes $n_1 = (p_{r_*}/r\Omega)^2$. Second, through the (discrete) choice of the argument used during the plunge to replace the variable x of the quasi-circular inspiral argument: *e.g.* either $x_\Omega \equiv (GM\Omega)^{2/3}$, or (following [90]) $x_\varphi \equiv v_\varphi^2 = (r_\omega\Omega)^2$ where $v_\varphi \equiv \Omega r_\omega$, and $r_\omega \equiv r[\psi(r, p_\varphi)]^{1/3}$ is a modified EOB radius, with ψ being defined as

$$\psi(r, p_\varphi) = \frac{2}{r^2} \left(\frac{dA(r)}{dr} \right)^{-1} \left[1 + 2v \left(\sqrt{A(r) \left(1 + \frac{p_\varphi^2}{r^2} \right)} - 1 \right) \right]. \quad (45)$$

For a given value of the symmetric mass ratio, and given values of the A -flexibility parameters $\tilde{a}_5(v), \tilde{a}_6(v)$ one can determine the values of the NQC parameters $a_i^{\ell m}$'s from accurate NR simulations of binary black hole coalescence (with mass ratio v) by imposing, say, that the complex EOB waveform $h_{\ell m}^{\text{EOB}}(t^{\text{EOB}}; \tilde{a}_5, \tilde{a}_6; a_i^{\ell m})$ *oscillates* the corresponding NR one $h_{\ell m}^{\text{NR}}(t^{\text{NR}})$ at their respective instants of “merger”, where $t_{\text{merger}}^{\text{EOB}} \equiv t_m^{\text{EOB}}$ was defined above (maximum of $\Omega^{\text{EOB}}(t)$), while $t_{\text{merger}}^{\text{NR}}$ is defined, say, as the (retarded) NR time where the modulus $|h_{22}^{\text{NR}}(t)|$ of the quadrupolar waveform reaches its maximum. The order of osculation that one requires between $h_{\ell m}^{\text{EOB}}(t)$ and $h_{\ell m}^{\text{NR}}(t)$ (or, separately, between their moduli and their phases or frequencies) depends on the number of NQC parameters $a_i^{\ell m}$. For instance, $a_1^{\ell m}$ and $a_2^{\ell m}$ affect only the modulus of $h_{\ell m}^{\text{EOB}}$ and allow one to match both $|h_{\ell m}^{\text{EOB}}|$ and its first time derivative, at merger, to their NR counterparts, while $a_3^{\ell m}, a_4^{\ell m}$ affect only the phase of the EOB waveform, and allow one to match the GW frequency $\omega_{\ell m}^{\text{EOB}}(t)$ and its first time derivative, at merger, to their NR counterparts. The above EOB/NR matching scheme has been developed and declined in various versions in Refs. [79, 80, 65, 87, 88, 91, 89, 77, 92]. One has also extracted the needed matching data from accurate NR simulations, and provided explicit, analytical v -dependent fitting formulas for them [65, 77, 92].

Having so “calibrated” the values of the NQC parameters by extracting non-perturbative information from a sample of NR simulations, one can then, for any choice of the A -flexibility parameters, compute a full EOB waveform (from early inspiral to late ringdown). The comparison of the latter NQC-completed EOB waveform to the results of NR simulations is discussed in the next Section.

5 EOB vs NR

There have been several different types of comparison between EOB and NR. For instance, the early work [81] pioneered the comparison between a purely analytical EOB waveform (uncalibrated to any NR information) and a NR waveform, while the early work [93] compared the predictions for the final spin of a coalescing black hole binary made by EOB, *completed* by the knowledge of the energy and angular momentum lost during ringdown by an extreme mass ratio binary (computed by the test-mass NR code of [94]), to comparable-mass NR simulations [95]. Since then, many other EOB/NR comparisons have been performed, both in the comparable-mass case [82, 86, 69, 79, 80, 65, 87], and in the small-mass-ratio case [68, 96, 97, 88, 89]. Note in this respect that the numerical simulations of the GW emission by extreme mass-ratio binaries have provided (and still provide) a very useful “laboratory” for learning about the motion and radiation of binary systems, and their description within the EOB formalism.

Here we shall discuss only two recent examples of EOB/NR comparisons, which illustrate different facets of this comparison.

5.1 EOB[NR] waveforms vs NR ones

We explained above how one could complete the EOB formalism by calibrating some of the natural EOB flexibility parameters against NR data. First, for any given mass ratio ν and any given values of the A -flexibility parameters $\tilde{a}_5(\nu), \tilde{a}_6(\nu)$, one can use NR data to uniquely determine the NQC flexibility parameters a_i 's. In other words, we have (for a given ν)

$$a_i = a_i[\text{NR data}; a_5, a_6],$$

where we defined a_5 and a_6 so that $\tilde{a}_5(\nu) = a_5\nu, \tilde{a}_6(\nu) = a_6\nu$. [We allow for some residual ν -dependence in a_5 and a_6 .] Inserting these values in the (analytical) EOB waveform then defines an NR-completed EOB waveform which still depends on the two unknown flexibility parameters a_5 and a_6 .

In Ref. [65] the (a_5, a_6) -dependent predictions made by such a NR-completed EOB formalism were compared to the high-accuracy waveform from an equal-mass binary black hole ($\nu = 1/4$) computed by the Caltech-Cornell-CITA group [98],

(and then made available on the web). It was found that there is a strong degeneracy between a_5 and a_6 in the sense that there is an excellent EOB-NR agreement for an extended region in the (a_5, a_6) -plane. More precisely, the phase difference between the EOB (metric) waveform and the Caltech-Cornell-CITA one, considered between GW frequencies $M\omega_L = 0.047$ and $M\omega_R = 0.31$ (i.e., the last 16 GW cycles before merger), stays smaller than 0.02 radians within a long and thin banana-like region in the (a_5, a_6) -plane. This “good region” approximately extends between the points $(a_5, a_6) = (0, -20)$ and $(a_5, a_6) = (-36, +520)$. As an example (which actually lies on the boundary of the “good region”), we shall consider here (following Ref. [99]) the specific values $a_5 = 0, a_6 = -20$ (to which correspond, when $\nu = 1/4$, $a_1 = -0.036347, a_2 = 1.2468$). [Ref. [65] did not make use of the NQC phase flexibility; i.e. it took $a_3 = a_4 = 0$. In addition, it used $n_2 = \ddot{r}/r\Omega^2$ and introduced a (real) modulus NQC factor $f_{\ell m}^{\text{NQC}}$ only for the dominant quadrupolar wave $\ell = 2 = m$.] We henceforth use M as time unit. This result relies on the proper comparison between NR and EOB time series, which is a delicate subject. In fact, to compare the NR and EOB phase time-series $\phi_{22}^{\text{NR}}(t_{\text{NR}})$ and $\phi_{22}^{\text{EOB}}(t_{\text{EOB}})$ one needs to shift, by additive constants, both one of the time variables, and one of the phases. In other words, we need to determine τ and α such that the “shifted” EOB quantities

$$t'_{\text{EOB}} = t_{\text{EOB}} + \tau, \quad \phi'_{22}{}^{\text{EOB}} = \phi_{22}^{\text{EOB}} + \alpha \quad (46)$$

“best fit” the NR ones. One convenient way to do so is first to “pinch” (i.e. constrain to vanish) the EOB/NR phase difference at two different instants (corresponding to two different frequencies ω_1 and ω_2). Having so related the EOB time and phase variables to the NR ones we can straightforwardly compare the EOB time series to its NR correspondent. In particular, we can compute the (shifted) EOB–NR phase difference

$$\Delta^{\omega_1, \omega_2} \phi_{22}^{\text{EOBNR}}(t_{\text{NR}}) \equiv \phi'_{22}{}^{\text{EOB}}(t'^{\text{EOB}}) - \phi_{22}^{\text{NR}}(t^{\text{NR}}). \quad (47)$$

Figure 2 compares⁹ (the real part of) the analytical EOB *metric* quadrupolar waveform $\Psi_{22}^{\text{EOB}}/\nu$ to the corresponding (Caltech-Cornell-CITA) NR *metric* waveform $\Psi_{22}^{\text{NR}}/\nu$. [Here, Ψ_{22} denotes the Zerilli-normalized asymptotic quadrupolar waveform, i.e. $\Psi_{22} \equiv \widehat{R}h_{22}/\sqrt{24}$ with $\widehat{R} = Rc^2/GM$.] This NR metric waveform has been obtained by a double time-integration (following the procedure of Ref. [80]) from the original, publicly available, *curvature* waveform ψ_4^{22} [98]. Such a curvature waveform has been extrapolated *both* in resolution and in extraction radius. The agreement between the analytical prediction and the NR result is striking, even around the merger. See Fig. 3 which closes up on the merger. The vertical line indicates the location of the EOB-merger time, i.e., the location of the maximum of the orbital frequency.

The phasing agreement between the waveforms is excellent over the full time span of the simulation (which covers 32 cycles of inspiral and about 6 cycles of ringdown), while the modulus agreement is excellent over the full span, apart from

⁹ The two “pinching” frequencies used for this comparison are $M\omega_1 = 0.047$ and $M\omega_2 = 0.31$.

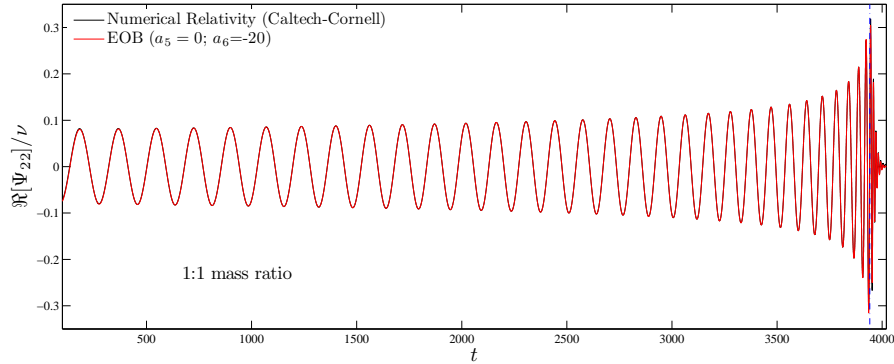


Fig. 2 This figure illustrates the comparison (made in Refs. [65, 99]) between the (NR-completed) EOB waveform (Zerilli-normalized quadrupolar ($\ell = m = 2$) metric waveform (42) with parameter-free radiation reaction (39) and with $a_5 = 0$, $a_6 = -20$) and one of the most accurate numerical relativity waveform (equal-mass case) nowadays available [98]. The phase difference between the two is $\Delta\phi \leq \pm 0.01$ radians during the entire inspiral and plunge, which is at the level of the numerical error.

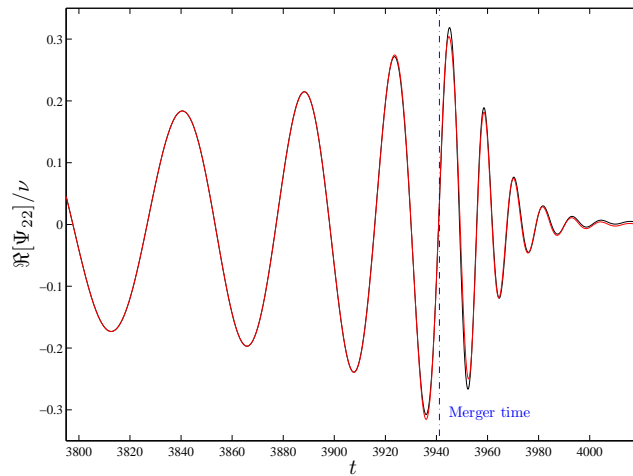


Fig. 3 Close up around merger of the waveforms of Fig. 2. Note the excellent agreement between *both* modulus and phasing also during the ringdown phase.

two cycles after merger where one can notice a difference. More precisely, the phase difference, $\Delta\phi = \phi_{\text{metric}}^{\text{EOB}} - \phi_{\text{metric}}^{\text{NR}}$, remains remarkably small ($\sim \pm 0.02$ radians) during the entire inspiral and plunge ($\omega_2 = 0.31$ being quite near the merger). By comparison, the root-sum of the various numerical errors on the phase (numerical truncation, outer boundary, extrapolation to infinity) is about 0.023 radians during the

inspiral [98]. At the merger, and during the ringdown, $\Delta\phi$ takes somewhat larger values ($\sim \pm 0.1$ radians), but it oscillates around zero, so that, on average, it stays very well in phase with the NR waveform whose error rises to ± 0.05 radians during ringdown. In addition, Ref. [65] compared the EOB waveform to accurate numerical relativity data (obtained by the Jena group [80]) on the coalescence of *unequal mass-ratio* black-hole binaries. Again, the agreement was good, and within the numerical error bars.

This type of high-accuracy comparison between NR waveforms and EOB[NR] ones (where EOB[NR] denotes a EOB formalism which has been completed by fitting some EOB-flexibility parameters to NR data) has been pursued and extended in Ref. [77]. The latter reference used the “improved” EOB formalism of Ref. [65] with some variations (*e.g.* a third modulus NQC coefficient a_i , two phase NQC coefficients, the argument $x_\Omega = (M\Omega)^{2/3}$ in $(\rho_{\ell m}^{\text{Taylor}}(x))^\ell$, eight QNM modes) and calibrated it to NR simulations of mass ratios $q = m_2/m_1 = 1, 2, 3, 4$ and 6 performed by the Caltech-Cornell-CITA group [100, 56]. They considered not only the leading $(\ell, m) = (2, 2)$ GW mode, but the subleading ones $(2, 1), (3, 3), (4, 4)$ and $(5, 5)$. They found that, for this large range of mass ratios, EOB[NR] (with suitably fitted, v -dependent values of a_5 and a_6) was able to describe the NR waveforms essentially within the NR errors. This confirms the usefulness of the EOB formalism in helping the detection and analysis of upcoming GW signals.

Here, having in view GW observations from ground-based interferometric detectors we focussed on comparable-mass systems. The EOB formalism has also been compared to NR results in the extreme mass-ratio limit $v \ll 1$. In particular, Ref. [88] found an excellent agreement between the analytical and numerical results.

5.2 EOB[3PN] dynamics vs NR one

Let us also mention other types of EOB/NR comparisons. Recently, two examples of EOB/NR comparisons have been performed directly at the level of the *dynamics* of a binary black hole, rather than at the level of the waveform. Moreover, contrary to the waveform comparisons of the previous subsection which involved an NR-completed EOB formalism (“EOB[NR]”), the dynamical comparisons we are going to discuss involve the purely analytical 3PN-accurate EOB formalism (“EOB[3PN]”), without any NR-based improvement.

First, Le Tiec et al. [83] have extracted from accurate NR simulations of slightly eccentric binary black-hole systems (for several mass ratios $q = m_1/m_2$ between $1/8$ and 1) the function relating the periastron-advance parameter

$$K = 1 + \frac{\Delta\Phi}{2\pi},$$

(where $\Delta\Phi$ is the periastron advance per radial period) to the dimensionless averaged angular frequency $M\Omega_\phi$ (with $M = m_1 + m_2$ as above). Then they compared

the NR-estimate of the mass-ratio dependent functional relation

$$K = K(M\Omega_\varphi; \nu),$$

where $\nu = q/(1+q)^2$, to the predictions of various analytic approximation schemes: PN theory, EOB theory and two different ways of using GSF theory. Let us only mention here that the prediction from the purely analytical EOB[3PN] formalism for $K(M\Omega_\varphi; \nu)$ [101] agreed remarkably well (essentially within numerical errors) with its NR estimate for all mass ratios, while, by contrast, the PN-expanded prediction for $K(M\Omega_\varphi; \nu)$ [70] showed a much poorer agreement, especially as q moved away from 1.

Second, Damour, Nagar, Pollney and Reisswig [84] have recently extracted from accurate NR simulations of black-hole binaries (with mass ratios $q = m_2/m_1 = 1, 2$ and 3) the gauge-invariant relation between the (reduced) binding energy $E = (\mathcal{E}^{\text{tot}} - M)/\mu$ and the (reduced) angular momentum $j = J/(G\mu M)$ of the system. Then they compared the NR-estimate of the mass-ratio dependent functional relation

$$E = E(j; \nu)$$

to the predictions of various analytic approximation schemes: PN theory and various versions of EOB theory (some of these versions were NR-completed). Let us only mention here that the prediction from the purely analytical, 3PN-accurate EOB[3PN] for $E(j; \nu)$ agreed remarkably well with its NR estimate (for all mass ratios) essentially *down to the merger*. This is illustrated in Fig. 4 for the $q = 1$ case. By contrast, the 3PN expansion in (powers of $1/c^2$) of the function $E(j; \nu)$ showed a much poorer agreement (for all mass ratios).

6 Other developments

6.1 EOB with spinning bodies

We lack space here for discussing the extension of the EOB formalism to binary systems made of spinning bodies. Let us start by mentioning that the spin-extension of the EOB formalism was initiated in Ref. [60], that the first EOB-based analytical calculation of a complete waveform from a spinning binary was performed in Ref. [61], and that the first attempt at calibrating a spinning EOB model to accurate NR simulations of spinning (non precessing) black-hole binaries was presented in [102]. In addition, several formal aspects related to the inclusion of spins in the EOB formalism have been discussed in Refs. [103, 104, 105, 106, 107] (see references within these papers for PN works dealing with spin effects) and a generalization of the factorized multipolar waveform of Ref. [64] to spinning, non-precessing binaries has been constructed in Refs. [76, 78].

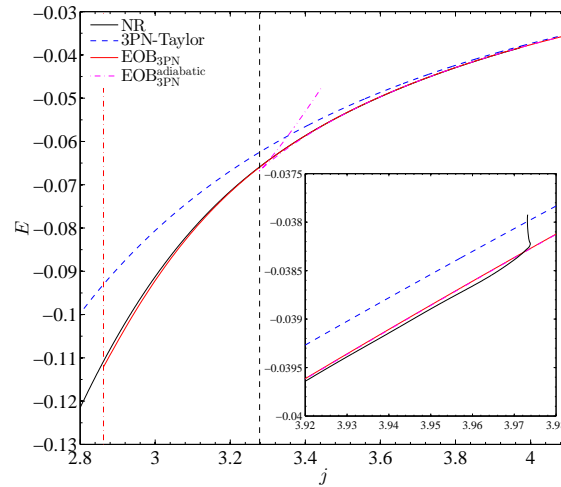


Fig. 4 Comparison (made in [84]) between various analytical estimates of the energy-angular momentum functional relation and its numerical-relativity estimate (equal-mass case). The standard “Taylor-expanded” 3PN $E(j)$ curve shows the largest deviation from NR results, especially at low j ’s, while the two (adiabatic and nonadiabatic) 3PN-accurate, *non-NR-calibrated* EOB $E(j)$ curves agree remarkably well with the NR one.

6.2 EOB with tidally deformed bodies

In binary systems comprising *neutron stars*, rather than black holes, the tidal deformation of the neutron star(s) will significantly modify the phasing of the emitted gravitational waveform during the late inspiral. As GW’s from binary neutron stars are expected sources for upcoming ground-based GW detectors, it is important to extend the EOB formalism by including tidal effects (see [108] and references therein). This extension has been defined in Refs. [109, 110]. The comparison between this tidal-extended EOB and state-of-the-art NR simulations of neutron-star binaries has been discussed in Refs. [111, 112]. It appears from these comparisons that the tidal-extended EOB formalism is able to describe the motion and radiation of neutron-star binaries within NR errors. More accurate simulations will be needed to ascertain whether one needs to calibrate some higher-order flexibility parameters of the tidal-EOB formalism, or whether the currently known analytic accuracy is sufficient.

6.3 EOB and GSF

We mentioned in the Introduction that GSF theory has recently opened a new source of information on the general relativistic two-body problem. Let us briefly mention here that there has been, recently, a quite useful transfer of information from GSF theory to EOB theory. The program of using GSF-theory to improve EOB-theory was first highlighted in Ref. [101]. That work pointed to several concrete gauge-invariant calculations (within GSF theory) that would provide accurate information about the $O(v)$ contributions to several EOB potentials. More precisely, let us define the functions $a(u)$ and $\bar{d}(u)$ as the v -linear contributions to the EOB potentials $A(u; v)$ and $\bar{D}(u; v) \equiv D^{-1}(u; v)$:

$$A(u; v) = 1 - 2u + v a(u) + O(v^2),$$

$$\bar{D}(u; v) = (AB)^{-1} = 1 + v \bar{d}(u) + O(v^2).$$

Ref. [101] has shown that a computation of the GSF-induced correction to the periastron advance of slightly eccentric orbits would allow one to compute the following combination of EOB functions

$$\bar{\rho}(u) = a(u) + u a'(u) + \frac{1}{2} u(1 - 2u) a''(u) + (1 - 6u) \bar{d}(u).$$

The GSF-calculation of the EOB function $\bar{\rho}(u)$ was then performed in Ref. [113] (in the range $0 \leq u \leq \frac{1}{6}$).

More recently, a series of works by Le Tiec and collaborators [114, 115, 116] have (through an indirect route) shown how GSF calculations could be used to compute the EOB v -linear $a(u)$ function separately from the $\bar{d}(u)$ one. Ref. [116] then gave a fitting formula for $a(u)$ over the interval $0 \leq u \leq \frac{1}{5}$ as well as accurate estimates of the coefficients of the Taylor expansion of $a(u)$ around $u = 0$ (corresponding to the knowledge of the PN expansion of $a(u)$ to a very high PN order). Very recently, Ackay et al. [117] succeeded in accurately computing (through GSF theory) the EOB $a(u)$ function over the larger interval $0 \leq u \leq \frac{1}{3}$. It was (surprisingly) found that $a(u)$ diverges like $a(u) \approx 0.25(1 - 3u)^{-1/2}$ at the light-ring limit $u \rightarrow (\frac{1}{3})^-$. The meaning for EOB theory of this singular behavior of $a(u)$ at the light-ring is discussed in detail in Ref. [117].

6.4 Toward further improvements to EOB

Let us finally mention some avenues for further progress in EOB theory.

Logarithmic contributions to the $A(u)$ and $\bar{D}(u)$ functions have been recently computed at the 4PN level [101, 118] and even the 5PN one [119, 116]. They have been incorporated in a recent, improved implementation of the EOB formalism [92].

Two groups have embarked on a calculation of the (full) conservative dynamics at the 4PN level [120, 121]. If they succeed, it will be important to translate their *gauge-dependent* results in the *gauge-invariant* form used in EOB theory. [Remember that EOB theory is essentially based on the gauge-invariant Delaunay Hamiltonian $H(I_a)$.]

More generally, let us emphasize that the EOB formalism provides a convenient, gauge-invariant way of packaging both the conservative dynamics and the multipolar waveform. This EOB packaging has often turned out to be very *economical*. We recommend that authors computing high-order PN corrections to either the dynamics or the waveform reexpress their results in terms of the EOB building blocks.

For instance, Jaranowski and Schaëfer [121] have recently given a partial result at 4PN, expressed in terms of the (gauge-invariant) function $E(M\Omega_\phi; \mathbf{v})$. In terms of this function, the 4PN contribution is a polynomial of the *fourth degree* in \mathbf{v} , namely, with $x \equiv (M\Omega_\phi)^{2/3}$ and

$$E(x; \mathbf{v}) = -\frac{1}{2}\mu c^2 x(1 + e_{1PN}(\mathbf{v})x + e_{2PN}(\mathbf{v})x^2 + e_{3PN}(\mathbf{v})x^3 + e_{4PN}(\mathbf{v}; \ln x)x^4 + O(x^5 \ln x)),$$

they found

$$e_{4PN}(\mathbf{v}; \ln x) = -\frac{3969}{128} + c_1 \mathbf{v} + c_2 \mathbf{v}^2 + \frac{301}{1728} \mathbf{v}^3 + \frac{77}{31104} \mathbf{v}^4 + \frac{448}{15} \mathbf{v} \ln x, \quad (48)$$

where they could not compute the values of the coefficients c_1 and c_2 of the terms linear and quadratic in \mathbf{v} , but only the contributions cubic and quartic in \mathbf{v} . We wish to point out that their result is re-expressed in a more economical (and more informative) way in terms of the basic EOB potential $A(u; \mathbf{v})$. Indeed, in terms of the PN expansion, of $A(u; \mathbf{v})$,

$$A^{\text{Taylor}}(u; \mathbf{v}) = 1 - 2u + \tilde{a}_3(\mathbf{v})u^3 + \tilde{a}_4(\mathbf{v})u^4 + \tilde{a}_5(\mathbf{v}; \ln u)u^5 + \tilde{a}_6(\mathbf{v}; \ln u)u^6 + \dots$$

the information contained in the above result can be entirely re-expressed in terms of the 4PN-level coefficient $\tilde{a}_5(\mathbf{v}; \ln u)$. When doing this re-expression, one then finds that the information content of Eq. (48) is that the 4PN-level EOB coefficient $\tilde{a}_5(\mathbf{v}; \ln u)$ is *no more than quadratic* in \mathbf{v} , i.e.

$$\tilde{a}_5(\mathbf{v}; \ln u) = (a_5 + \frac{64}{5} \ln u) \mathbf{v} + a'_5 \mathbf{v}^2,$$

without contributions of degree \mathbf{v}^3 and \mathbf{v}^4 . We recall that similar cancellations of higher \mathbf{v}^n terms were found at lower PN orders in the EOB $A(u; \mathbf{v})$ function. Namely, they were found to contain only terms *linear* in \mathbf{v} , while $\tilde{a}_3(\mathbf{v})$ could a priori have been quadratic in \mathbf{v} , and $\tilde{a}_4(\mathbf{v})$ could a priori have been cubic in \mathbf{v} . The fact that similar remarkable cancellations still hold, according to the result of [121], at the 4PN level, is a clear indication that the EOB packaging of information of the

dynamics in the $A(u; nu)$ potential is quite compact. Indeed, it says that the two complicated terms $\frac{301}{1728}v^3 + \frac{77}{31104}v^4$ in the energy function are already encoded in the structure of the EOB formalism. Finally, note that the full gauge-invariant content of a 4PN computation of the dynamics, when interpreted within the EOB formalism, is described by only three EOB terms: the coefficient $\tilde{a}_5(v; \ln u)$ in $A(u; v)$, an analogous coefficient $\tilde{d}_4(v; \ln u)$ in $\bar{D}(u; v)$, and an additional contribution to $Q(p)$.

Regarding the waveform, let us mention another recent example where it would have been useful and clarifying to use the EOB packaging. Namely, when re-expressing it in terms of the factorized EOB waveform, the new content of the recent 3.5PN level computation by Faye, Marsat, Blanchet, and Iyer [122] of the PN-expanded quadrupolar waveform h_{22} , is entirely contained in an additional 3.5PN-level contribution to the supplementary phase, namely $\delta_{22} = (30995/1134v + 962/135v^2)x^{7/2}$. Indeed, the 3.5PN-level contributions to the modulus computed in [122] were already included in the factorized EOB waveform of Ref. [65].

7 Conclusions

We hope that this brief review has made it clear that:

1. There is a *complementarity* between the various current approaches to the general relativistic two-body problem: post-Newtonian, Effective One Body, gravitational self-force and numerical relativity simulations (of both comparable-mass and extreme-mass-ratio systems).
2. The effective one body formalism offers a convenient framework for combining, in a synergetic manner, information coming from the other approaches. This formalism seems to constitute an efficient way to analytically describe the motion and radiation of circularized¹⁰ binaries, and to provide accurate gravitational wave templates for detection and data analysis.
3. The general relativistic two-body problem is more lively than ever. It provides an example of Poincaré’s sentence: “Il n’y a pas de problèmes résolus, il y a seulement des problèmes plus ou moins résolus.” [“There are no (definitely) solved problems, there are only more-or-less solved problems.”]

References

1. T. Damour, *The problem of motion in Newtonian and Einsteinian gravity*, in *Three Hundred years of Gravitation*, ed. by S.W. Hawking, W. Israel (Cambridge University Press, Cambridge, 1987), pp. 128–198

¹⁰ See [73] for a recent extension of the EOB formalism to non-circular (ellipticlike or hyperboliclike) motions.

2. T. Damour, *Gravitational radiation and the motion of compact bodies*, in *Gravitational Radiation*, ed. by N. Deruelle, T. Piran (North-Holland, Amsterdam, 1983), pp. 59–144
3. P. Jaranowski, G. Schäfer, *Third post-Newtonian higher order ADM Hamilton dynamics for two-body point-mass systems*, Phys. Rev. D **57**, 7274 (1998). Erratum: *ibid.* **63**, 029902 (2001)
4. L. Blanchet, G. Faye, *General relativistic dynamics of compact binaries at the third post-Newtonian order*, Phys. Rev. D **63**, 062005 (2001)
5. T. Damour, P. Jaranowski, G. Schäfer, *Dimensional regularization of the gravitational interaction of point masses*, Phys. Lett. B **513**, 147 (2001)
6. L. Blanchet, T. Damour, G. Esposito-Farèse, *Dimensional regularization of the third post-Newtonian dynamics of point particles in harmonic coordinates*, Phys. Rev. D **69**, 124007 (2004)
7. Y. Itoh, T. Futamase, *New derivation of a third post-Newtonian equation of motion for relativistic compact binaries without ambiguity*, Phys. Rev. D **68**, 121501 (2003)
8. M.E. Pati, C.M. Will, *Post-Newtonian gravitational radiation and equations of motion via direct integration of the relaxed Einstein equations. II: Two-body equations of motion to second post-Newtonian order, and radiation-reaction to 3.5 post-Newton*, Phys. Rev. D **65**, 104008 (2002)
9. C. Königsdorffer, G. Faye, G. Schäfer, *The binary black-hole dynamics at the third-and-a-half post-Newtonian order in the ADM-formalism*, Phys. Rev. D **68**, 044004 (2003)
10. S. Nissanke, L. Blanchet, *Gravitational radiation reaction in the equations of motion of compact binaries to 3.5 post-Newtonian order*, Class. Quant. Grav. **22**, 1007 (2005)
11. L. Blanchet, T. Damour, *Radiative gravitational fields in general relativity I. General structure of the field outside the source*, Philos. Trans. R. Soc. London, Ser. A **320**, 379 (1986)
12. L. Blanchet, T. Damour, *Post-Newtonian generation of gravitational waves*, Ann. Inst. Henri Poincaré A **50**, 377 (1989)
13. T. Damour, B.R. Iyer, *Multipole analysis for electromagnetism and linearized gravity with irreducible cartesian tensors*, Phys. Rev. D **43**, 3259 (1991)
14. T. Damour, B.R. Iyer, *Post-Newtonian generation of gravitational waves. II. The spin moments*, Ann. Inst. Henri Poincaré A **54**, 115 (1991)
15. L. Blanchet, T. Damour, *Hereditary effects in gravitational radiation*, Phys. Rev. D **46**, 4304 (1992)
16. L. Blanchet, *Second-post-Newtonian generation of gravitational radiation*, Phys. Rev. D **51**, 2559 (1995)
17. C.M. Will, A.G. Wiseman, *Gravitational radiation from compact binary systems: gravitational waveforms and energy loss to second post-Newtonian order*, Phys. Rev. D **54**, 4813 (1996)
18. C.M. Will, *Generation of post-Newtonian gravitational radiation via direct integration of the relaxed Einstein equations*, Prog. Theor. Phys. Suppl. **136**, 158 (1999)
19. M.E. Pati, C.M. Will, *Post-Newtonian gravitational radiation and equations of motion via direct integration of the relaxed Einstein equations. I: Foundations*, Phys. Rev. D **62**, 124015 (2000)
20. R. Epstein, R.V. Wagoner, *Post-Newtonian generation of gravitational waves*, Astrophys. J. **197**, 717 (1975)
21. K.S. Thorne, *Multipole expansions of gravitational radiation*, Rev. Mod. Phys. **52**, 299 (1980)
22. R.V. Wagoner, C.M. Will, *Post-Newtonian gravitational radiation from orbiting point masses*, Astrophys. J. **210**, 764 (1976)
23. A.G. Wiseman, *Coalescing binary systems of compact objects to (post)⁵-Newtonian order. IV. The gravitational wave tail*, Phys. Rev. D **48**, 4757 (1993)
24. L. Blanchet, G. Schäfer, *Gravitational wave tails and binary star systems*, Class. Quantum Grav. **10**, 2699 (1993)
25. L. Blanchet, T. Damour, B.R. Iyer, C.M. Will, A.G. Wiseman, *Gravitational-radiation damping of compact binary systems to second post-Newtonian order*, Phys. Rev. Lett. **74**, 3515 (1995)

26. L. Blanchet, T. Damour, B.R. Iyer, *Gravitational waves from inspiralling compact binaries: Energy loss and waveform to second-post-Newtonian order*, Phys. Rev. D **51**, 5360 (1995). Erratum: *ibid.* **54**, 1860 (1996)
27. L. Blanchet, *Gravitational-wave tails of tails*, Class. Quantum Grav. **15**, 113 (1998). Erratum *ibid.* **22**, 3381 (2005)
28. L. Blanchet, B.R. Iyer, B. Joguet, *Gravitational waves from inspiralling compact binaries: Energy flux to third post-Newtonian order*, Phys. Rev. D **65**, 064005 (2002). Erratum: *ibid.* **71**, 129903 (2005)
29. L. Blanchet, B.R. Iyer, *Hadamard regularization of the third post-Newtonian gravitational wave generation of two point masses*, Phys. Rev. D **71**, 024004 (2005)
30. L. Blanchet, T. Damour, G. Esposito-Farèse, B.R. Iyer, *Gravitational radiation from inspiralling compact binaries completed at the third post-Newtonian order*, Phys. Rev. Lett. **93**, 091101 (2004)
31. L. Blanchet, T. Damour, G. Esposito-Farèse, B.R. Iyer, *Dimensional regularization of the third post-Newtonian gravitational wave generation from two point masses*, Phys. Rev. D **71**, 124004 (2005)
32. L. Blanchet, *Quadrupole-quadrupole gravitational waves*, Class. Quantum Grav. **15**, 89 (1998)
33. E. Berti, V. Cardoso, J.A. Gonzalez, et al., *Inspiral, merger and ringdown of unequal mass black hole binaries: A multipolar analysis*, Phys. Rev. D **76**, 064034 (2007)
34. L.E. Kidder, *Using full information when computing modes of post-Newtonian waveforms from inspiralling compact binaries in circular orbit*, Phys. Rev. D **77**, 044016 (2008)
35. L. Blanchet, G. Faye, B.R. Iyer, S. Sinha, *The third post-Newtonian gravitational wave polarisations and associated spherical harmonic modes for inspiralling compact binaries in quasi-circular orbits*, Class. Quantum Grav. **25**, 165003 (2008)
36. L. Blanchet, *Gravitational radiation from post-Newtonian sources and inspiralling compact binaries*, Living Rev. Relativity **5**, lrr-2002-3 (2002). URL <http://www.livingreviews.org/lrr-2002-3>
37. E. Poisson, *Gravitational radiation from a particle in circular orbit around a black hole. I. Analytic results for the nonrotating case*, Phys. Rev. D **47**, 1497 (1993)
38. M. Sasaki, *Post-Newtonian expansion of the ingoing-wave Regge-Wheeler function*, Prog. Theor. Phys **92**, 17 (1994)
39. H. Tagoshi, M. Sasaki, *Post-Newtonian expansion of gravitational waves from a particle in circular orbit around a Schwarzschild black hole*, Prog. Theor. Phys **92**, 745 (1994)
40. T. Tanaka, H. Tagoshi, M. Sasaki, *Gravitational waves by a particle in circular orbit around a Schwarzschild black hole*, Prog. Theor. Phys **96**, 1087 (1996)
41. M. Sasaki, H. Tagoshi, *Analytic black hole perturbation approach to gravitational radiation*, Living Rev. Relativity **6**, lrr-2003-6 (2003). URL <http://www.livingreviews.org/lrr-2003-6>
42. S. Foffa, R. Sturani, *Effective field theory calculation of conservative binary dynamics at third post-Newtonian order*, Phys. Rev. D **84**, 044031 (2011)
43. W.D. Goldberger, I.Z. Rothstein, *An effective field theory of gravity for extended objects*, Phys. Rev. D **73**, 104029 (2006)
44. T. Damour, G. Esposito-Farèse, *Tensor multiscalar theories of gravitation*, Class. Quantum Grav. **9**, 2093 (1992)
45. T. Damour, G. Esposito-Farèse, *Testing gravity to second post-Newtonian order: A field theory approach*, Phys. Rev. D **53**, 5541 (1996)
46. T. Damour, G. Esposito-Farèse, *Gravitational-wave versus binary-pulsar tests of strong-field gravity*, Phys. Rev. D **58**, 042001 (1998)
47. W.D. Goldberger, A. Ross, *Gravitational radiative corrections from effective field theory*, Phys. Rev. D **81**, 124015 (2010)
48. F. Pretorius, *Evolution of binary black hole spacetimes*, Phys. Rev. Lett. **95**, 121101 (2005)
49. M. Campanelli, C.O. Lousto, P. Marronetti, Y. Zlochower, *Accurate evolutions of orbiting black-hole binaries without excision*, Phys. Rev. Lett. **96**, 111101 (2006)

50. J.G. Baker, J. Centrella, D.I. Choi, M. Koppitz, J. van Meter, *Gravitational wave extraction from an inspiraling configuration of merging black holes*, Phys. Rev. Lett. **96**, 111102 (2006)
51. M. Boyle, D.A. Brown, L.E. Kidder, et al., *High-accuracy comparison of numerical relativity simulations with post-Newtonian expansions*, Phys. Rev. D **76**, 124038 (2007)
52. F. Pretorius, *Binary Black Hole Coalescence*, in *Physics of Relativistic Objects in Compact Binaries: From Birth to Coalescence*, Astrophysics and Space Science Library, vol. 359, ed. by M. Colpi, et al. (Springer/Canopus Publishing Limited, Dordrecht; Bristol, 2009), pp. 305–370
53. L. Barack, *Gravitational self force in extreme mass-ratio inspirals*, Class. Quantum Grav. **26**, 213001 (2009)
54. M. Hannam, S. Husa, U. Sperhake, B. Bruegmann, J.A. Gonzalez, *Where post-Newtonian and numerical-relativity waveforms meet*, Phys. Rev. D **77**, 044020 (2008)
55. M. Hannam, S. Husa, B. Bruegmann, A. Gopakumar, *Comparison between numerical-relativity and post-Newtonian waveforms from spinning binaries: the orbital hang-up case*, Phys. Rev. D **78**, 104007 (2008)
56. I. MacDonald, A.H. Mroué, H.P. Pfeiffer, et al., *Suitability of hybrid gravitational waveforms for unequal-mass binaries*, Phys. Rev. D **87**, 024009 (2013)
57. A. Buonanno, T. Damour, *Effective one-body approach to general relativistic two-body dynamics*, Phys. Rev. D **59**, 084006 (1999)
58. A. Buonanno, T. Damour, *Transition from inspiral to plunge in binary black hole coalescences*, Phys. Rev. D **62**, 064015 (2000)
59. T. Damour, P. Jaranowski, G. Schäfer, *On the determination of the last stable orbit for circular general relativistic binaries at the third post-Newtonian approximation*, Phys. Rev. D **62**, 084011 (2000)
60. T. Damour, *Coalescence of two spinning black holes: An effective one-body approach*, Phys. Rev. D **64**, 124013 (2001)
61. A. Buonanno, Y. Chen, T. Damour, *Transition from inspiral to plunge in precessing binaries of spinning black holes*, Phys. Rev. D **74**, 104005 (2006)
62. E. Brézin, C. Itzykson, J. Zinn-Justin, *Relativistic balmer formula including recoil effects*, Phys. Rev. D **1**, 2349 (1970)
63. T. Damour, B.R. Iyer, B.S. Sathyaprakash, *Improved filters for gravitational waves from inspiralling compact binaries*, Phys. Rev. D **57**, 885 (1998)
64. T. Damour, B.R. Iyer, A. Nagar, *Improved resummation of post-Newtonian multipolar waveforms from circularized compact binaries*, Phys. Rev. D **79**, 064004 (2009)
65. T. Damour, A. Nagar, *An improved analytical description of inspiralling and coalescing black-hole binaries*, Phys. Rev. D **79**, 081503 (2009)
66. M. Davis, R. Ruffini, J. Tiomno, *Pulses of gravitational radiation of a particle falling radially into a Schwarzschild black hole*, Phys. Rev. D **5**, 2932 (1972)
67. R.H. Price, J. Pullin, *Colliding black holes: The close limit*, Phys. Rev. Lett. **72**, 3297 (1994)
68. T. Damour, A. Nagar, *Faithful Effective-One-Body waveforms of small-mass-ratio coalescing black-hole binaries*, Phys. Rev. D **76**, 064028 (2007)
69. T. Damour, A. Nagar, *Comparing Effective-One-Body gravitational waveforms to accurate numerical data*, Phys. Rev. D **77**, 024043 (2008)
70. T. Damour, P. Jaranowski, G. Schäfer, *Dynamical invariants for general relativistic two-body systems at the third post-Newtonian approximation*, Phys. Rev. D **62**, 044024 (2000)
71. T. Damour, P. Jaranowski, G. Schäfer, *Poincaré invariance in the ADM Hamiltonian approach to the general relativistic two-body problem*, Phys. Rev. D **62**, 021501 (2000). Erratum: *ibid.* D **63**, 029903 (2000)
72. T. Damour, G. Schäfer, *Higher order relativistic periastron advances and binary pulsars*, Nuovo Cimento B **101**, 127 (1988)
73. D. Bini, T. Damour, *Gravitational radiation reaction along general orbits in the effective one-body formalism*, Phys. Rev. D **86**, 124012 (2012)
74. R. Fujita, B.R. Iyer, *Spherical harmonic modes of 5.5 post-Newtonian gravitational wave polarisations and associated factorised resummed waveforms for a particle in circular orbit around a Schwarzschild black hole*, Phys. Rev. D **82**, 044051 (2010)

75. R. Fujita, *Gravitational radiation for extreme mass ratio inspirals to the 14th post-Newtonian order*, Prog. Theor. Phys. **127**, 583 (2012)
76. Y. Pan, A. Buonanno, R. Fujita, E. Racine, H. Tagoshi, *Post-Newtonian factorized multipolar waveforms for spinning, non-precessing black-hole binaries*, Phys. Rev. D **83**, 064003 (2011)
77. Y. Pan, A. Buonanno, M. Boyle, et al., *Inspiral-merger-ringdown multipolar waveforms of nonspinning black-hole binaries using the effective-one-body formalism*, Phys. Rev. D **84**, 124052 (2011)
78. A. Taracchini, Y. Pan, A. Buonanno, et al., *Prototype effective-one-body model for non-precessing spinning inspiral-merger-ringdown waveforms*, Phys. Rev. D **86**, 024011 (2012)
79. T. Damour, A. Nagar, E.N. Dorband, D. Pollney, L. Rezzolla, *Faithful Effective-One-Body waveforms of equal-mass coalescing black-hole binaries*, Phys. Rev. D **77**, 084017 (2008)
80. T. Damour, A. Nagar, M. Hannam, S. Husa, B. Bruegmann, *Accurate Effective-One-Body waveforms of inspiralling and coalescing black-hole binaries*, Phys. Rev. D **78**, 044039 (2008)
81. A. Buonanno, G.B. Cook, F. Pretorius, *Inspiral, merger and ring-down of equal-mass black-hole binaries*, Phys. Rev. D **75**, 124018 (2007)
82. Y. Pan, A. Buonanno, J.G. Baker, et al., *A data-analysis driven comparison of analytic and numerical coalescing binary waveforms: Nonspinning case*, Phys. Rev. D **77**, 024014 (2008)
83. A. Le Tiec, A.H. Mroue, L. Barack, et al., *Periastron advance in black hole binaries*, Phys. Rev. Lett. **107**, 141101 (2011)
84. T. Damour, A. Nagar, D. Pollney, C. Reisswig, *Energy versus angular momentum in black hole binaries*, Phys. Rev. Lett. **108**, 131101 (2012)
85. T. Damour, E. Gourgoulhon, P. Grandclément, *Circular orbits of corotating binary black holes: Comparison between analytical and numerical results*, Phys. Rev. D **66**, 024007 (2002)
86. A. Buonanno, Y. Pan, J.G. Baker, et al., *Toward faithful templates for non-spinning binary black holes using the effective-one-body approach*, Phys. Rev. D **76**, 104049 (2007)
87. A. Buonanno, Y. Pan, H.P. Pfeiffer, et al., *Effective-one-body waveforms calibrated to numerical relativity simulations: coalescence of non-spinning, equal-mass black holes*, Phys. Rev. D **79**, 124028 (2009)
88. S. Bernuzzi, A. Nagar, A. Zenginoglu, *Binary black hole coalescence in the extreme-mass-ratio limit: testing and improving the effective-one-body multipolar waveform*, Phys. Rev. D **83**, 064010 (2011)
89. E. Barausse, A. Buonanno, S.A. Hughes, et al., *Modeling multipolar gravitational-wave emission from small mass-ratio mergers*, Phys. Rev. D **85**, 024046 (2012)
90. T. Damour, A. Gopakumar, *Gravitational recoil during binary black hole coalescence using the effective one body approach*, Phys. Rev. D **73**, 124006 (2006)
91. S. Bernuzzi, A. Nagar, A. Zenginoglu, *Binary black hole coalescence in the large-mass-ratio limit: the hyperboloidal layer method and waveforms at null infinity*, Phys. Rev. D **84**, 084026 (2011)
92. T. Damour, A. Nagar, S. Bernuzzi, *Improved effective-one-body description of coalescing nonspinning black-hole binaries and its numerical-relativity completion*, ArXiv e-prints [arXiv:1212.4357 [gr-qc]] (2012)
93. T. Damour, A. Nagar, *Final spin of a coalescing black-hole binary: an Effective-One-Body approach*, Phys. Rev. D **76**, 044003 (2007)
94. T. Damour, A. Nagar, A. Tartaglia, *Binary black hole merger in the extreme mass ratio limit*, Class. Quantum Grav. **24**, S109 (2007)
95. J.A. Gonzalez, U. Sperhake, B. Bruegmann, M. Hannam, S. Husa, *Total recoil: the maximum kick from nonspinning black-hole binary inspiral*, Phys. Rev. Lett. **98**, 091101 (2007)
96. N. Yunes, A. Buonanno, S.A. Hughes, M.C. Miller, Y. Pan, *Modeling extreme mass ratio inspirals within the effective-one-body approach*, Phys. Rev. Lett. **104**, 091102 (2010)
97. N. Yunes, A. Buonanno, S.A. Hughes, et al., *Extreme mass-ratio inspirals in the effective-one-body approach: Quasi-circular, equatorial orbits around a spinning black hole*, Phys. Rev. D **83**, 044044 (2011)

98. M.A. Scheel, M. Boyle, T. Chu, et al., *High-accuracy waveforms for binary black hole inspiral, merger, and ringdown*, Phys. Rev. D **79**, 024003 (2009)
99. T. Damour, A. Nagar, *The Effective One-Body Description of the Two-Body Problem*, in *Mass and Motion in General Relativity, Fundamental Theories of Physics*, vol. 162, ed. by L. Blanchet, A. Spallicci, B. Whiting (Springer, Berlin; New York, 2011), pp. 211–252
100. L.T. Buchman, H.P. Pfeiffer, M.A. Scheel, B. Szilágyi, *Simulations of non-equal mass black hole binaries with spectral methods*, Phys. Rev. D **86**, 084033 (2012)
101. T. Damour, *Gravitational self force in a Schwarzschild background and the Effective One Body formalism*, Phys. Rev. D **81**, 024017 (2010)
102. Y. Pan, A. Buonanno, L.T. Buchman, et al., *Effective-one-body waveforms calibrated to numerical relativity simulations: coalescence of non-precessing, spinning, equal-mass black holes*, Phys. Rev. D **81**, 084041 (2010)
103. T. Damour, P. Jaranowski, G. Schäfer, *Effective one body approach to the dynamics of two spinning black holes with next-to-leading order spin-orbit coupling*, Phys. Rev. D **78**, 024009 (2008)
104. E. Barausse, E. Racine, A. Buonanno, *Hamiltonian of a spinning test-particle in curved spacetime*, Phys. Rev. D **80**, 104025 (2009). Erratum: *ibid.* D **85**, 069904 (2012)
105. E. Barausse, A. Buonanno, *An improved effective-one-body Hamiltonian for spinning black-hole binaries*, Phys. Rev. D **81**, 084024 (2010)
106. A. Nagar, *Effective one body Hamiltonian of two spinning black-holes with next-to-next-to-leading order spin-orbit coupling*, Phys. Rev. D **84**, 084028 (2011)
107. E. Barausse, A. Buonanno, *Extending the effective-one-body Hamiltonian of black-hole binaries to include next-to-next-to-leading spin-orbit couplings*, Phys. Rev. D **84**, 104027 (2011)
108. T. Damour, A. Nagar, L. Villain, *Measurability of the tidal polarizability of neutron stars in late-inspiral gravitational-wave signals*, Phys. Rev. D **85**, 123007 (2012)
109. T. Damour, A. Nagar, *Effective One Body description of tidal effects in inspiralling compact binaries*, Phys. Rev. D **81**, 084016 (2010)
110. D. Bini, T. Damour, G. Faye, *Effective action approach to higher-order relativistic tidal interactions in binary systems and their effective one body description*, Phys. Rev. D **85**, 124034 (2012)
111. L. Baiotti, T. Damour, B. Giacomazzo, A. Nagar, L. Rezzolla, *Analytic modelling of tidal effects in the relativistic inspiral of binary neutron stars*, Phys. Rev. Lett. **105**, 261101 (2010)
112. L. Baiotti, T. Damour, B. Giacomazzo, A. Nagar, L. Rezzolla, *Accurate numerical simulations of inspiralling binary neutron stars and their comparison with effective-one-body analytical models*, Phys. Rev. D **84**, 024017 (2011)
113. L. Barack, T. Damour, N. Sago, *Precession effect of the gravitational self-force in a Schwarzschild spacetime and the effective one-body formalism*, Phys. Rev. D **82**, 084036 (2010)
114. A. Le Tiec, L. Blanchet, B.F. Whiting, *The first law of binary black hole mechanics in general relativity and post-Newtonian theory*, Phys. Rev. D **85**, 064039 (2012)
115. A. Le Tiec, E. Barausse, A. Buonanno, *Gravitational self-force correction to the binding energy of compact binary systems*, Phys. Rev. Lett. **108**, 131103 (2012)
116. E. Barausse, A. Buonanno, A. Le Tiec, *The complete non-spinning effective-one-body metric at linear order in the mass ratio*, Phys. Rev. D **85**, 064010 (2012)
117. S. Akcay, L. Barack, T. Damour, N. Sago, *Gravitational self-force and the effective-one-body formalism between the innermost stable circular orbit and the light ring*, Phys. Rev. D **86**, 104041 (2012)
118. L. Blanchet, S.L. Detweiler, A. Le Tiec, B.F. Whiting, *High-order post-Newtonian fit of the gravitational self-force for circular orbits in the Schwarzschild geometry*, Phys. Rev. D **81**, 084033 (2010)
119. T. Damour, (2010). (unpublished); cited in Ref. [113], which quoted and used some combinations of the logarithmic contributions to $a(u)$ and $\bar{d}(u)$
120. S. Foffa, R. Sturani, *The dynamics of the gravitational two-body problem at fourth post-Newtonian order and at quadratic order in the Newton constant* *The dynamics of the gravitational two-body problem at fourth post-Newtonian order and at quadratic order in the Newton constant*, ArXiv e-prints [arXiv:1206.7087 [gr-qc]] (2012)

121. P. Jaranowski, G. Schäfer, *Towards the 4th post-Newtonian Hamiltonian for two-point-mass systems*, Phys. Rev. D **86**, 061503 (2012)
122. G. Faye, S. Marsat, L. Blanchet, B.R. Iyer, *The third and a half post-Newtonian gravitational wave quadrupole mode for quasi-circular inspiralling compact binaries*, Class. Quantum Grav. **29**, 175004 (2012)